

This discussion paper is/has been under review for the journal Atmospheric Chemistry and Physics (ACP). Please refer to the corresponding final paper in ACP if available.

Source identification and budget analysis on elevated levels of formaldehyde within ship plumes: a photochemical/dynamic model analysis

C. H. Song¹, H. S. Kim¹, R. von Glasow², P. Brimblecombe², J. Kim³, R. J. Park⁴, and J. H. Woo⁵

¹School of Environmental Science and Engineering, Gwangju Institute of Science and Technology (GIST), Gwangju, 500-712, Korea

²School of Environmental Sciences, University of East Anglia, Norwich, NR4 7TJ, UK

³Department of Atmospheric Sciences, Yonsei University, Seoul, 120-749, Korea

⁴School of Environmental Sciences, Seoul National University, Seoul, 151-742, Korea

⁵Department of Advanced Technology Fusion, Konkuk University, Seoul, 143-701, Korea

Received: 4 May 2010 – Accepted: 2 June 2010 – Published: 23 June 2010

Correspondence to: C. H. Song (chsong@gist.ac.kr)

Published by Copernicus Publications on behalf of the European Geosciences Union.

Elevated HCHO levels in the ship-going MBL

C. H. Song et al.

Title Page

Abstract

Introduction

Conclusions

References

Tables

Figures

◀

▶

◀

▶

Back

Close

Full Screen / Esc

Printer-friendly Version

Interactive Discussion



Abstract

Elevated levels of formaldehyde (HCHO) along the ship corridors have been observed by satellite sensors, such as ESA/ERS-2 GOME (Global Ozone Monitoring Experiment), and were also predicted by global 3-D chemistry-transport models. In this study, three likely sources of the elevated HCHO levels were investigated to identify the detailed sources and examine the contributions of the sources (budget) of the elevated levels of HCHO in the ship corridors using a newly-developed ship-plume photochemical/dynamic model: (1) primary HCHO emission from ships; (2) secondary HCHO production via the atmospheric oxidation of Non-methane volatile organic compounds (NMVOCs) emitted from ships; and (3) atmospheric oxidation of CH₄ within the ship plumes. From multiple ship-plume model simulations, CH₄ oxidation by elevated levels of in-plume OH radicals was found to be the main factor responsible for the elevated levels of HCHO in the ship corridors. More than ~91% of the HCHO for the base ship plume case (ITCT 2K2 ship-plume case) is produced by this atmospheric chemical process, except in the areas close to the ship stacks where the main source of the elevated HCHO levels would be primary HCHO from the ships (due to the deactivation of CH₄ oxidation from the depletion of in-plume OH radicals). Because of active CH₄ oxidation (chemical destruction of CH₄) by OH radicals, the instantaneous chemical lifetime of CH₄ (τ_{CH_4}) decreased to ~0.45 yr inside the ship plume, which is in contrast to τ_{CH_4} of ~1.1 yr in the background (up to ~41% decrease). A variety of likely ship-plume situations at three locations at different latitudes within the global ship corridors was also studied to determine the extent of the enhancements in the HCHO levels in the marine boundary layer (MBL) influenced by ship emissions. It was found that the ship-plume HCHO levels could be 20.5–434.9 pptv higher than the background HCHO levels depending on the latitudinal locations of the ship plumes (i.e., intensity of solar radiation and temperature), MBL stability and NO_x emission rates. On the other hand, NMVOC emissions from ships were not found to be a primary source of photochemical HCHO production inside ship plumes due to their rapid and individual dilution. However, the

Elevated HCHO levels in the ship-going MBL

C. H. Song et al.

Title Page

Abstract

Introduction

Conclusions

References

Tables

Figures

◀

▶

◀

▶

Back

Close

Full Screen / Esc

Printer-friendly Version

Interactive Discussion



diluted NMVOCs would contribute to the HCHO productions in the background air. The greater impact of ship-plume photochemistry on the atmospheric MBL oxidation cycles, global climate, and marine eco-system in the global ship corridors are also discussed based on the results in this study.

1 Introduction

Recently, ship emissions have attracted increasing attention because it is becoming obvious that ship-emitted NO_x , SO_2 and particles can perturb the atmospheric photochemical cycles and global radiation budget significantly in the marine boundary layer (MBL) (Corbett and Fischbeck, 1997, 1999; Capaldo et al., 1999; Lawrence and Crutzen, 1999; Kasibhatla et al., 2000; Song et al., 2003a,b; Endresen et al., 2003; Eyring et al., 2007; Hoor et al., 2009; Kim et al., 2009). Until now, many detailed analyses of the impacts of the ocean-going ship emissions on atmospheric MBL chemistry and the global radiation budget have been carried out in a range of aspects: (1) $\text{O}_3/\text{HO}_x/\text{NO}_y$ photochemistry in the MBL (e.g., Lawrence and Crutzen, 1999; Endresen et al., 2003; Song et al., 2003a; von Glasow et al., 2003; Kim et al., 2009); (2) sulfur cycle in the MBL (e.g., Capaldo et al., 1999; Song et al., 2003b; Faloona, 2009); and (3) impacts on the global radiation budget (e.g., Capaldo et al., 1999; Endresen et al., 2003; Phinney et al., 2009).

More recently, elevated levels of HCHO in heavy ship-traffic corridors (or large HCHO vertical columns over the oceans impacted by ship emissions) were detected by the ESA/ERS-2 GOME (Global Ozone Monitoring Experiment) sensor (Marbach et al., 2009). The elevated HCHO levels along the heavy ship-traffic corridors are of fundamental importance because they can greatly perturb the atmospheric oxidation cycle (or $\text{O}_3/\text{HO}_x/\text{N}_x\text{O}_y$ photochemistry) in ship-influenced MBL. In turn, the perturbed oxidation cycle can also affect the global radiation budget, for example, by possibly enhancing the O_3 mixing ratios in the MBL. Moreover, if the main source of MBL HCHO production is from atmospheric CH_4 oxidation, the removal of CH_4 can also indicate re-

Elevated HCHO levels in the ship-going MBL

C. H. Song et al.

Title Page

Abstract

Introduction

Conclusions

References

Tables

Figures

◀

▶

◀

▶

Back

Close

Full Screen / Esc

Printer-friendly Version

Interactive Discussion



duced atmospheric warming, as CH₄ is a major global warming gas (Hansen and Sato, 2001; IPCC, 2007). According to global chemistry-transport modeling (CTM) studies by Bey et al. (2001) and Lawrence et al. (2001), approximately ~50% of the global CH₄ chemical losses is removed within the planetary and marine boundary layers (PBL and MBL), even when ship NO_x emissions are not considered. The model-predicted fractions of global CH₄ destruction in the MBL could be even higher if ~21% of the anthropogenic global NO_x emissions from ocean-going ships are considered (cf. Corbett and Koehler, 2003). Recently, Hoor et al. (2009), in their multiple global 3-D CTM ensemble study, reported active CH₄ destruction within the TBL. However, their study was carried out without rigorous consideration of the complexity and non-linearity of ship-plume photochemistry in the global CTM simulations. Overall, it is important to understand such marine boundary chemical processes in terms of the atmospheric photochemistry and chemistry-climate interactions.

Another important issue that should be addressed is the possible levels of HCHO in ship-influenced MBL. It is difficult to retrieve accurate HCHO mixing ratios in the MBL from satellite sensors, such as GOME, SCIAMACHY, and OMI, mainly because of (1) difficulty in accurately estimating the air-mass factor (AMF) and (2) interference by ship-emitted aerosols during the retrieval of HCHO columns over the heavy ship-traffic ocean corridors (Marbach et al., 2009). Hence, there is some controversy regarding the HCHO levels within the heavy ship traffic corridors (Marbach et al., 2009). Considering these arguments, in this numerical analysis of ship-plume photochemistry, an attempt was made to answer two important scientific questions: (1) what is the main (or dominant) atmospheric HCHO generation process, and (2) how much can HCHO be generated or the HCHO mixing ratios increases by the atmospheric HCHO generation processes within the ship plumes?

In order to explore these issues, first of all, three likely sources of the elevated HCHO levels in the ship plumes were assumed and then examined: (1) primary HCHO emission from ships; (2) secondary HCHO production via the atmospheric oxidation of Non-methane volatile organic compounds (NMVOCs) emitted from ships; and (3) atmo-

Elevated HCHO levels in the ship-going MBL

C. H. Song et al.

Title Page

Abstract

Introduction

Conclusions

References

Tables

Figures

◀

▶

◀

▶

Back

Close

Full Screen / Esc

Printer-friendly Version

Interactive Discussion



spheric oxidation of CH₄ within the ship plumes. A ship-plume photochemical/dynamic model developed previously by Kim et al. (2009) was used to help answer to these scientific questions. In addition, in terms of the ship-plume photochemical/dynamic model development and its applications, this is a companion study of Kim et al. (2009) with particular focus on ship-plume HCHO. This study first discusses the ship-plume case from the Intercontinental Transport and Chemical Transformation 2002 (ITCT 2K2) campaign as a base study case because this case has been analyzed most thoroughly (hereafter, called “ITCT 2K2 ship-plume case”), and various likely ship-plume cases at different latitudinal locations of the global ship tracks (hereafter, these are called “constructed cases”) were then explored. The impacts of the ship-plume photochemistry on the MBL photochemical cycles, global climate, and marine eco-system in the global ship corridors are further discussed based on the discussions in this study.

2 Model description

UBoM 2K8 (Utility photochemical Box Model 2008) was used in this numerical modeling study. The UBoM 2K8 model has three operational modes for atmospheric photochemical modeling: (1) Lagrangian backward/forward trajectory photochemical modeling (Song et al., 2007); (2) Eulerian photochemical modeling (Tuan, 2008); and (3) ship-plume photochemical/dynamic modeling (Song et al., 2003a,b; Kim et al., 2009). Although the UBoM 2K8 model has three operational modes, the three modes share the same gas-phase photochemistry, heterogeneous reaction schemes, and aerosol physics and dynamics. In this study, the last photochemical modeling mode was used.

2.1 Model validation

The details of the ship-plume modeling components of the UBoM 2K8 model were explained previously by Song et al. (2003a,b) and Kim et al. (2009), and are not repeated here. However, the model has two fundamental components to treat: (1) atmospheric

Elevated HCHO levels in the ship-going MBL

C. H. Song et al.

Title Page

Abstract

Introduction

Conclusions

References

Tables

Figures

◀

▶

◀

▶

Back

Close

Full Screen / Esc

Printer-friendly Version

Interactive Discussion



thermo-chemical, photo-chemical and heterogeneous reactions; and (2) turbulent dispersion of air pollutants emitted from a ship. For the latter, a “Gaussian-based” turbulent dispersion scheme was adopted from the Offshore and Coastal Dispersion (OCD) model with some modifications (Hanna et al., 1985; Song et al., 2003a; Kim et al., 2009). For the former, a modified Lurmann chemical mechanism was used, in which 255 atmospheric gas-phase reactions coupled to heterogeneous condensations and aerosol micro-physics were considered (Lurmann et al., 1986; Song et al., 2003b). In particular, several turbulent ship-plume dispersion schemes within the MBL were reviewed extensively by Faloona (2009). According to his study, the parameterizations from the OCD model would be the best for accurately describing the turbulent dispersion of ship plumes within the MBL, which was confirmed by Kim et al. (2009) using the ITCT 2K2 ship-plume case.

Along with the turbulent dispersion scheme, the full capability of the ship-plume photochemical/dynamic model was validated comprehensively using a data set from the ITCT 2K2 ship-plume measurements by comparing the model-predicted data with the aircraft-measured ship-plume concentrations of NO_x , NO_y , O_3 , HNO_3 , and H_2SO_4 as well as the ozone production efficiency (OPE) (Parrish et al., 2004; Kim et al., 2009; Xuan et al., 2009). Figure 1 shows a schematic diagram of the airborne ship-plume experiment using NOAA WP-3D aircraft during the ITCT 2K2 campaign, which were carried out approximately 100 km off the coast of California. The NOAA WP-3D aircraft traversed the ship-plume eight times from transects A to H at an angle of 59° between the ship-plume centerline and the flight pathways. In Fig. 1, A^- and A^+ represent two imaginary transects where the ship-plume photochemistry near the ship stack is intended to be investigated. According to Kim et al. (2009), the ship-plume photochemical/dynamic model can predict the ship-plume composition accurately. This was confirmed again in Fig. 2 with further multiple sensitivity model runs, in which the NO_x emission rates from the ship were varied over a range of $2.6\text{--}13.3\text{ g s}^{-1}$, together with the primary NMVOC and HCHO emissions (both the primary NMVOC and HCHO emissions are discussed further in Sect. 2.2). As shown in Fig. 2, there is good agreement

**Elevated HCHO levels
in the ship-going
MBL**

C. H. Song et al.

Title Page

Abstract

Introduction

Conclusions

References

Tables

Figures

◀

▶

◀

▶

Back

Close

Full Screen / Esc

Printer-friendly Version

Interactive Discussion



between the model-predicted and observed concentrations of NO_x , O_3 , and HNO_3 . For this set of model validations, the concentrations of one primary pollutant (NO_x) and two secondary species (O_3 and HNO_3) were compared because the photochemistry of these three species is coupled closely with one another and is also related strongly to the production of OH radicals, which play a key role in CH_4 and NMVOC oxidation in the MBL. Here, the blue and red shadows represent the ranges of the model-predicted species concentrations under moderately stable and stable MBL conditions, respectively. Further details regarding the measurement uncertainties, selection of the MBL stability, and data analysis were discussed previously by Kim et al. (2009).

2.2 Model simulations

According to Chen et al. (2005), the ship being investigated in this study was equipped with a 6,707 kW engine. With this power, the total rate of NMVOC emission from the ship can be estimated to be 0.93 g s^{-1} using the NMVOC emission factor of 0.5 g kWh^{-1} reported by European Commission Directorate General Environment and Entec UK Ltd. (2005; hereafter, abbreviated ECDGE & Entec). On the other hand, the total NMVOC emission rate from the ship can also be estimated from a ratio of NO_x to NMVOCs in the ship emissions. Again, according to ECDGE & Entec (2005), the ratio was typically 29.6:1.0 (NO_x :NMVOCs) on a mass basis. Total NMVOC emission rates of 0.09 – 0.45 g s^{-1} were obtained from the estimated NO_x emission rate from the ship (2.6 to 13.3 g s^{-1}). From these estimations, the total NMVOC emission rate could range between 0.09 g s^{-1} and 0.93 g s^{-1} . Although the estimated values have significant uncertainty, they appear to be consistent with the globally-averaged ship NMVOC emission rate of 0.75 g s^{-1} estimated by Endresen et al. (2003). Table 1 was constructed from these values. In Table 1, the chemical speciation and fraction of NMVOCs emitted from the ship were determined from the ship-plume data reported by Cooper et al. (1996), EPA (2000), Endresen et al. (2003), ECDGE & Entec (2005), and Houyoux (2005). The fraction of primary HCHO in the NMVOC emissions varies

Elevated HCHO levels in the ship-going MBL

C. H. Song et al.

Title Page

Abstract

Introduction

Conclusions

References

Tables

Figures



Back

Close

Full Screen / Esc

Printer-friendly Version

Interactive Discussion



considerably from ship to ship, fuel-type, age of the ship, engine-speed etc. HCHO fractions of 0.4–10.0% were reported based on the Lloyd Register (1995), EPA (2000), Houyoux (2005), and Marbach et al. (2009). Unless noted otherwise, the mid-point values from Table 1 were used (making their summation unity) in this numerical study of the ship-plume photochemical/dynamic modeling.

As discussed by Kim et al. (2009), the ship-plume dispersion is governed primarily by the stability class of MBL. Based on the NOAA WP-3D aircraft measurements of the meteorological variables in/around the ship plume, Kim et al. (2009) suggested that the stability class of the ship-going MBL would range from moderately stable (E) to stable (F). In general situations, within the heavy ship-traffic MBL over the remote oceans, the stability class of the MBL frequently ranges from neutral (D) to stable (F) (cf. Frick and Hoppel, 2000; Song et al., 2003a). Therefore, three stability classes (instead of the two stability classes for the base case study) were considered in this numerical ship-plume photochemistry study of the constructed cases at different latitudinal locations: (1) neutral (D); (2) moderately stable (E); and (3) stable (F) stability classes.

In this numerical ship-plume modeling study, a background photochemical box model was also run to consider the diurnal changes in HCHO mixing ratios in the background air using both the background meteorological conditions and chemical composition. This calculation was carried out by running the background photochemical box model until a pseudo steady-state in the background chemical composition had been reached. The background HCHO mixing ratios calculated were then mixed with the ship-plume volumes. By doing this, a discontinuity problem in HCHO mixing ratios, which typically occurs at the interface between the edge of the ship-plumes and the background air, can be avoided. With the exception of HCHO, the fixed average concentrations measured by the NOAA WP-3D aircraft in the background were used in the model simulations.

One of the key issues of this study is CH₄ oxidation. The CH₄ oxidation rates are controlled mainly by the levels of OH radicals, which were found to be a function of the stability class of the MBL (Song et al., 2003a; Kim et al., 2009). The levels of

Elevated HCHO levels in the ship-going MBL

C. H. Song et al.

Title Page

Abstract

Introduction

Conclusions

References

Tables

Figures

◀

▶

◀

▶

Back

Close

Full Screen / Esc

Printer-friendly Version

Interactive Discussion



OH radicals can also be affected by several other factors, such as NO_x emission rate, NMVOC emission rates, NMVOC chemical speciation, and ship location. As discussed above, there is some uncertainty in the ship NO_x emission rates, which would range from 2.6 g s^{-1} to 13.3 g s^{-1} in the base ship-plume case (Chen et al., 2005; Kim et al., 2009). In addition, in general the NO_x emission rates from ships must vary from ship to ship, ship-type, ship-speed and engine-type (cf. EPA, 2000; ECDGE & Entec, 2005; Houyoux, 2005). As discussed previously, the total NMVOC emission rates were also variable, and there is large uncertainty, even in the chemical speciation of NMVOCs emitted from ships (see Table 1). Moreover, the OH radical mixing ratios are a strong function of the meteorological variables, such as solar radiation, relative humidity and temperature (Song et al., 2003a,b). Therefore, in order to consider these situations, several cases were constructed by changing the factors that can affect the OH levels within the ship plumes. The cases are presented in Sect. 3.2. For example, the most active/vigorous ship-plume photochemistry would be expected in the “stable, tropical MBL” with large NO_x emission rates, producing the highest OH levels. This study first discusses the ITCT 2K2 ship-plume case as a base study case, and then explores various likely constructed cases at different latitudinal locations. The results from the constructed case studies are discussed in Sect. 3.2.

3 Results and discussions

In this section, the budget of HCHO within the ITCT 2K2 ship-plume as a base case was first examined because this ITCT 2K2 ship-plume was analyzed most thoroughly by Chen et al. (2005) and Kim et al. (2009) (Sect. 3.1). The ship-plume photochemical/dynamic model was then applied to locations at other latitudes (i.e., ship tracks in tropical, subtropical, and mid-latitude regions) to determine the possible extent of the increase in HCHO levels (or degree of activity of the HCHO-related photochemistry) within the global ship corridors (Sect. 3.2).

Elevated HCHO levels in the ship-going MBL

C. H. Song et al.

Title Page

Abstract

Introduction

Conclusions

References

Tables

Figures

◀

▶

◀

▶

Back

Close

Full Screen / Esc

Printer-friendly Version

Interactive Discussion



3.1 Base-case study

As mentioned in Sect. 1, the following three possible sources of the elevated HCHO levels were considered in this numerical study: (1) primary HCHO emission from ships; (2) secondary HCHO production via atmospheric oxidation of NMVOCs emitted from ships; and (3) atmospheric oxidations of CH₄ within the ship plumes. Of these three possible sources, the last source, CH₄ oxidation, may be significant.

In theory, two atmospheric reactions could initiate photochemical HCHO production via the atmospheric CH₄ oxidation: (1) CH₄+OH ((R1) in Table 2) and (2) CH₄+O(¹D) (with two reaction pathways, refer to (R2) and (R3) in Table 2). Of these three reactions, the latter two would be of secondary importance because O(¹D) radicals mainly react with the more abundant H₂O molecules in the MBL, producing OH radicals (i.e., O(¹D)+H₂O → 2OH). The former could be primarily responsible for photochemical HCHO production within the MBL. Numerical sensitivity analyses of the reactions (i.e., switching the reactions ON and OFF) were carried out to determine the impact of the reactions on HCHO production in the ship-going MBL.

Background HCHO mixing ratios of approximately 210–430 pptv were reported in the MBL, e.g. over the Southern Indian Ocean (SIO) by Wagner et al. (2001). In addition, enhanced OH concentrations due to ship NO_x emissions were suggested by several global CTM simulation studies (e.g., Lawrence and Crutzen, 1999; Hoor et al., 2009). Although both measurement and modeling studies can provide circumstantial evidence for the possibility of active HCHO production or generation in a ship-going MBL, they are limited in that: (1) the measurements were made only over a limited location like the SIO; and (2) such Eulerian modeling framework with a coarse grid resolution tends to over-predict the OH radical concentrations by skipping the complex, non-linear in-plume photochemistry. Therefore, it can produce excessive CH₄ oxidation by OH radicals (Lawrence and Crutzen, 1999; Song et al., 2003a; von Glasow et al., 2003; Kim et al., 2009). In this numerical study, a single, ordinary ship-plume situation was considered, focusing more on how fast the CH₄ and/or NMVOCs can

Elevated HCHO levels in the ship-going MBL

C. H. Song et al.

Title Page

Abstract

Introduction

Conclusions

References

Tables

Figures

◀

▶

◀

▶

Back

Close

Full Screen / Esc

Printer-friendly Version

Interactive Discussion



be oxidized and how much the HCHO mixing ratios can be enhanced from the CH₄ and/or NMVOCs oxidation or by direct HCHO ship emissions inside the single ship-plume. The implications of this work in the global atmospheric photochemistry within a ship-going MBL are then discussed.

Figure 3 shows the budget of HCHO generation (photochemical production+direct emission) inside the ship plume of the ITCT 2K2 ship-plume case. In Fig. 3, four cases were considered: (CASE I) CH₄+OH reaction ON inside the ship-plume; (CASE II) CH₄+OH reaction ON+NMVOC emission without primary HCHO emission; (CASE III) CH₄+OH reaction ON+NMVOC emission with primary HCHO emission; and (Background): only with the HCHO background mixing ratios. As shown in Fig. 3, neither the direct emission of HCHO from the ship nor atmospheric oxidation of NMVOCs emitted from the ship is the major factor that can completely explain the elevated levels of HCHO within the ship plume. Instead, the enhanced rate of the atmospheric oxidation of CH₄ is the most likely cause for the enhanced HCHO levels. Figure 3a and b, the first and the second rows in Fig. 3, present the changes in the transect-averaged ship-plume HCHO mixing ratios with respect to the ship-plume travel time (Fig. 3a, first row) and differences between the averaged ship-plume HCHO mixing ratios and model-predicted background HCHO mixing ratios (Fig. 3b, second row), respectively. Both the transect-averaged ship-plume HCHO mixing ratios and the differences are a function of the stability class of the MBL. In other words, both ship-plume HCHO mixing ratios and their differences increase as the MBL changes from neutral (D) to stable (F). The increases are due mainly to the atmospheric CH₄ oxidation (see CASE I in Fig. 3). The increased CH₄ oxidation is certainly due to the increased OH radical concentrations inside the ship plume (this will be shown in Fig. 5).

In addition, there was almost no difference between CASEs I and II. Although the “total NMVOC” emission rates are up to 5% of the ship NO_x emission rates in the simulations, the emission rates of the “individual” NMVOC species in the model simulations (refer to Table 1) are small because they are chemically-lumped (or chemically-split) into eight individual NMVOC species in the simulations. The relatively low emissions

Elevated HCHO levels in the ship-going MBL

C. H. Song et al.

Title Page

Abstract

Introduction

Conclusions

References

Tables

Figures

◀

▶

◀

▶

Back

Close

Full Screen / Esc

Printer-friendly Version

Interactive Discussion



of the individual NMVOCs are then diluted rapidly and concurrently, resulting in minimal impacts of NMVOC emissions from the ship. More importantly, the dilution of NMVOCs actually occurs in the early ship-plume stage, where oxidation is not yet very active due to the depletion of OH radicals (this will be discussed further below). Due to these two reasons, the simulations with and without NMVOC emissions (CASEs I and II) produced similar results. In this sense, ship-emitted NMVOCs are not responsible for the HCHO enhancements “inside the ship plumes”. However, the diluted NMVOCs would contribute to HCHO production “in the background air”. Wagner et al. (2002) reported that approximately ~22.7% of HCHO could be produced from the background NMVOCs over the SIO.

Here, there are two important issues, particularly near the ship stack (approximately, within the ship-plume travel time of ~50 min): (1) the levels of the transect-averaged ship-plume HCHO are below the background HCHO levels near the ship stack (CASE I and II) and (2) the primary HCHO emitted from the ship could make a significant contribution to the levels of the averaged ship-plume HCHO (CASE III). The former is basically due to ozone titration near the ship stack. The ozone titration near the ship stack is well-known and has been discussed in many papers (e.g., Song et al., 2003a; von Glasow et al., 2003; Kim et al., 2009). Ozone titration then leads to OH depletion near the ship stack, and causes an imbalance between HCHO production and destruction inside the ship plume (i.e., HCHO production rate \ll HCHO destruction rate). Therefore, the levels of HCHO near the ship stack fall below the background HCHO levels inside the ship plume (hereafter, called “HCHO depletion”). However, when the primary HCHO emission from the ship is considered (CASE III, the most realistic case), the primary HCHO compensates for the depletion of HCHO near the ship stack and the HCHO levels decrease in a pseudo-exponential manner. These dynamic changes in the HCHO budget are certainly due to the “non-linear” characteristics of the ship-plume photochemistry.

In order to analyze the HCHO budget in more detail for CASE III (the most realistic case), the fractions of the ship-plume HCHO mixing ratios and enhanced ship-plume

Elevated HCHO levels in the ship-going MBL

C. H. Song et al.

[Title Page](#)[Abstract](#)[Introduction](#)[Conclusions](#)[References](#)[Tables](#)[Figures](#)[⏪](#)[⏩](#)[◀](#)[▶](#)[Back](#)[Close](#)[Full Screen / Esc](#)[Printer-friendly Version](#)[Interactive Discussion](#)

HCHO mixing ratios are depicted in Fig. 3c and d, the third and the fourth rows in Fig. 3, respectively. As shown in Fig. 3c and d, until a ship-plume travel time of ~ 20 min, primary HCHO emission is the main source of the HCHO enhancement inside the ship plume. The primary HCHO contributes continuously to ship-plume HCHO generation until ~ 50 min after the ship puff is released. However, CH_4 oxidation becomes the major contributor after a ship-plume travel time of ~ 50 min. In particular, after a ship-plume travel time of 100 min, almost all the HCHO enhancement is due to atmospheric CH_4 oxidation.

Figure 4 shows the cross-sectional profiles of the HCHO mixing ratios in the ITCT 2K2 ship-plume at ten transects (including two imaginary transects A^- and A^0). Two issues should be noted in Fig. 4: (1) the contribution of primary HCHO emissions to HCHO in the cross-sectional HCHO profiles of the ship plume depends strongly on the stability of the MBL and (2) the cross-sectional profiles of the HCHO mixing ratios initially show a minimum in the plume core; the duration of this effect depends on the stability of the MBL. Again, these “non-Gaussian” HCHO profiles across the ship plume are important evidence of the non-linear ship-plume photochemistry (Kim et al., 2009). The contribution of primary HCHO to the total HCHO profiles last longer, as the MBL becomes more stable. The non-Gaussian shapes of the cross-sectional HCHO profiles also last longer as the MBL becomes more stable (because ship plumes are spread more narrowly when the MBL becomes more stable, as shown in Fig. 4). However, as ship-plume ages photochemically and dynamically, the cross-sectional HCHO profiles become Gaussian and the contribution of primary HCHO to the profiles of HCHO mixing ratios reaches a minimum. In addition, the extent of the enhancements of the HCHO levels increases, as the MBL becomes more stable. For example, the peak HCHO mixing ratios are elevated above the background HCHO levels by ~ 170 pptv (at transect F) under stable MBL conditions, whereas they are elevated only by ~ 70 pptv (at transect D) under neutral conditions. These enhancements in the HCHO levels were used in Sect. 3.2 as an indicator of the degree of activity of the HCHO-related photochemistry inside the ship plume.

Elevated HCHO levels in the ship-going MBL

C. H. Song et al.

[Title Page](#)[Abstract](#)[Introduction](#)[Conclusions](#)[References](#)[Tables](#)[Figures](#)[⏪](#)[⏩](#)[◀](#)[▶](#)[Back](#)[Close](#)[Full Screen / Esc](#)[Printer-friendly Version](#)[Interactive Discussion](#)

Figure 5 represents the OH radical concentrations, instantaneous chemical lifetime of CH₄ (τ_{CH_4}), and the net instantaneous HCHO production rate (P_{HCHO}) at ten ship-plume transects under moderately stable MBL conditions. The quantities in Fig. 5 were defined as follows:

$$D_{\text{CH}_4} = \{k_1[\text{OH}] + k_2[\text{O}(^1\text{D})] + k_3[\text{O}(^1\text{D})]\}[\text{CH}_4] \quad (1)$$

$$D_{\text{HCHO}} = \{J_1 + J_2 + k_4[\text{OH}] + k_5[\text{NO}_3] + k_6[\text{O}(^3\text{P})]\}[\text{HCHO}] \quad (2)$$

$$F_{\text{HCHO}} \approx D_{\text{CH}_4} + \sum_i \Phi_i k_{\text{NMVOCs},i} [\text{OH}][\text{NMVOCs}]_i - k_7[\text{CH}_3\text{O}_2][\text{HO}_2] - k_8[\text{CH}_3\text{O}_2]^2 \quad (3)$$

$F_{\text{HCHO}} \approx D_{\text{CH}_4}$, when

$$D_{\text{CH}_4} \gg \sum_i \Phi_i k_{\text{NMVOCs},i} [\text{OH}][\text{NMVOCs}]_i \quad \text{and}$$

$$D_{\text{CH}_4} \gg k_7[\text{CH}_3\text{O}_2][\text{HO}_2] + k_8[\text{CH}_3\text{O}_2]^2 \quad (3-1)$$

$$\tau_{\text{CH}_4} = \frac{[\text{CH}_4]}{D_{\text{CH}_4}} \quad (4)$$

where k_i are the thermal reaction rate constants ($\text{cm}^3 \text{molecules}^{-1} \text{s}^{-1}$), and the values for k_i are shown in Table 2. $k_{\text{NMVOCs},i}$ and Φ_i are the reaction rate constant ($\text{cm}^3 \text{molecules}^{-1} \text{s}^{-1}$) for HCHO production from the oxidation of NMVOC species i by OH radicals and the HCHO yield from the oxidation of NMVOC species i , respectively. D_{CH_4} , D_{HCHO} , and F_{HCHO} denote the rates of CH₄ and HCHO destruction and HCHO formation, respectively. Another possible oxidation reaction of CH₄ would be CH₄+Cl in the MBL (Sander and Crutzen, 1996; Vogt et al., 1996; Wagner et al., 2002; von Glasow et al., 2003). However, these reactions were not considered in this study because there was no clear evidence of halogen-mediated photochemistry found in this specific ship-plume case (Parrish et al., 2004; Chen et al., 2005; Kim et al., 2009).

**Elevated HCHO levels
in the ship-going
MBL**

C. H. Song et al.

Title Page

Abstract

Introduction

Conclusions

References

Tables

Figures

◀

▶

◀

▶

Back

Close

Full Screen / Esc

Printer-friendly Version

Interactive Discussion



Elevated HCHO levels in the ship-going MBL

C. H. Song et al.

Title Page

Abstract

Introduction

Conclusions

References

Tables

Figures

◀

▶

◀

▶

Back

Close

Full Screen / Esc

Printer-friendly Version

Interactive Discussion



As discussed above, CH_4 is destroyed/oxidized, producing HCHO directly and/or CH_3O_2 radicals indirectly. CH_3O_2 radicals are converted to HCHO via (R11) and (R12), as shown in Table 2 (Finlayson-Pitts and Pitts, 2000; Wagner et al., 2002). Both CH_3OOH and CH_3OH are also eventually converted to HCHO via (R8) and (R9) in Table 2. However, the production rates of both “reservoir” species (CH_3OOH and CH_3OH) were subtracted from the HCHO production rate (F_{HCHO}) due to the long chemical lifetimes of both species and the relatively short time period of the ship-plume photochemical/dynamic modeling (see Eq. 3). However, the ship-plume situations inherently create high NO_x conditions (HO_x -limited situations), which limits the formation of the both reservoir species. Therefore, under such high NO_x conditions, one mole of CH_4 produces one mole of HCHO, and at a pseudo steady-state, the rates of CH_4 destruction are approximately equal to the rates of HCHO production, as expressed in Eq. (3-1), when $D_{\text{CH}_4} \gg \sum_i \Phi_i k_{\text{NMVOCs},i} [\text{OH}] [\text{NMVOCs}]_i$. As discussed previously, HCHO production from NMVOC oxidation inside the ship plume is also minor compared to that from CH_4 oxidation (D_{CH_4}), due to the rapid and concurrent individual species dilutions and the OH radical deletion. This was confirmed in Fig. 6.

In the current framework of the analysis, two points should be considered: (1) the changes in the quantities inside and outside the ship-plume; and (2) the imbalance between D_{CH_4} ($\approx F_{\text{HCHO}}$) and D_{HCHO} inside the ship plume. The former was examined to compare the characteristics of CH_4 destruction and HCHO formation inside and outside the ship-plume. In the latter, the difference between F_{HCHO} and D_{HCHO} can be regarded as the net instantaneous HCHO production rate (P_{HCHO}), i.e.:

$$P_{\text{HCHO}} \approx F_{\text{HCHO}} - D_{\text{HCHO}} \approx D_{\text{CH}_4} - D_{\text{HCHO}} \quad (5)$$

Figure 6 compares the two net transect-averaged instantaneous HCHO production rates (P_{HCHO}) for the three MBL stability conditions. The black solid and red dashed lines represent the two P_{HCHO} expressions defined by $D_{\text{CH}_4} - D_{\text{HCHO}}$ and $F_{\text{HCHO}} - D_{\text{HCHO}}$ in Eq. (5), respectively. The two lines show the differences around the peak P_{HCHO} values. However, the differences are not large (up to $\sim 17\%$ at the peak

Elevated HCHO levels in the ship-going MBL

C. H. Song et al.

Title Page

Abstract

Introduction

Conclusions

References

Tables

Figures

◀

▶

◀

▶

Back

Close

Full Screen / Esc

Printer-friendly Version

Interactive Discussion



$\overline{P_{\text{HCHO}}}$ values under the stable MBL condition, see Fig. 6(c)). Here, the differences between $D_{\text{CH}_4} - D_{\text{HCHO}}$ and $F_{\text{HCHO}} - D_{\text{HCHO}}$ around the plume travel times of 20–70 min indicate the influences of the term, $\sum_i \Phi_i k_{\text{NMVOCs},i} [\text{OH}] [\text{NMVOCs}]_i$, in Eq. (3), whereas the slight differences after a plume travel time $> \sim 100$ min (black solid line > red dashed line) are caused by the triggered radical terminations (i.e., CH_3OOH and CH_3OH formations, (R9) and (R10) in Table 2). This is because the ship plume encounters relatively low NO_x conditions in this ship-plume photochemical stage due to dilution. On the other hand, the negative $\overline{P_{\text{HCHO}}}$ values until ~ 20 min after the ship plume is released indicate net HCHO destruction, mainly via active (R4) and (R5) in Table 2, which are due to OH depletion during the early ship-plume photochemical stage.

Figure 5 presents the cross-sectional variations of the quantities defined in Eqs. (1)–(5). They vary depending on the stability classes of the MBL. However, their general characteristics are similar. Therefore, only the results from the moderately stable MBL case are shown in Fig. 5. First of all, the peak OH radical concentrations increase, even up to $\sim 1.7 \times 10^7$ molecules cm^{-3} . These levels of OH radicals are ~ 2.8 times higher than the background levels of OH ($\sim 6.1 \times 10^6$ molecules cm^{-3} , also refer to Chen et al, 2005), indicating ~ 2.8 times faster atmospheric CH_4 oxidation inside the ship plume than that in the background (out-plume) MBL. This was confirmed in terms of τ_{CH_4} . τ_{CH_4} is approximately ~ 1.1 yr in the background, but as low as ~ 0.45 yr inside the ship plume. τ_{CH_4} at the peak of the ship plume was approximately $\sim 41\%$ lower than τ_{CH_4} in the background under the moderately stable MBL conditions. Under stable MBL conditions, τ_{CH_4} was shortened even further (not shown). Here, it should be emphasized once again that τ_{CH_4} is a function of the OH radical concentration. Our ship-plume model simulations can successfully regenerate, e.g., ~ 8 yr of CH_4 lifetime (approximately, globally-averaged value at daytime), when the OH radical concentration is 1.02×10^6 molecules cm^{-3} , as reported from the Oslo global CTM simulation by Karlsdóttir and Isaksen (2000).

As mentioned above, the imbalance between D_{CH_4} ($\approx F_{\text{HCHO}}$) and D_{HCHO} (i.e., P_{HCHO}) inside the ship plume was also examined. Basically, it is the imbalance that enhances

the ship-plume HCHO levels (or depletion of the HCHO mixing ratios close to the ship stack). As shown in Fig. 5, P_{HCHO} inside the ship plume has values above the background P_{HCHO} , indicating excessive HCHO formation inside the ship plume. The background P_{HCHO} ranges from ~ 0.02 to ~ 0.03 pptv s $^{-1}$, whereas the ship-plume P_{HCHO} increases up to ~ 0.08 pptv s $^{-1}$. Such an imbalance leads to large increases in the HCHO levels inside the ship plume, as shown in Fig. 4. However, some depletion at the ship-plume center is also found near the ship locations between transects A $^{-}$ and B. Again, this is due mainly to the retarded F_{HCHO} caused by OH depletion. Figure 7 shows the time-dependent changes in the transect-averaged OH radical concentrations ($[\text{OH}]$), net instantaneous transect-averaged chemical lifetime of CH $_4$ ($\overline{\tau_{\text{CH}_4}}$), and net instantaneous transect-averaged HCHO production rate ($\overline{P_{\text{HCHO}}}$) under moderately stable and stable MBL conditions. All values shown in Fig. 7 were averaged over the transects of the ship plume. In Fig. 7, one could also find a very dynamic, non-linear nature of the ship-plume photochemistry. Near the ship stack, both $[\text{OH}]$ and $\overline{P_{\text{HCHO}}}$ are very low, whereas $\overline{\tau_{\text{CH}_4}}$ are high. However, as ship plume travels, $[\text{OH}]$ recovers and $\overline{P_{\text{HCHO}}}$ increases accordingly. In contrast, $\overline{\tau_{\text{CH}_4}}$ decreases. Then, after 50–80 min, both $[\text{OH}]$ and $\overline{P_{\text{HCHO}}}$ decrease again.

3.2 Constructed case studies

The ship-plume HCHO photochemistry was investigated using the base-case ship plume (ITCT 2K2 ship plume). The investigation was extended to various ship-track situations by applying the ship-plume photochemical/dynamic model to heavy ship-traffic corridors at three different latitudinal locations in the world. To accomplish this, thirty six possible scenarios were constructed by changing three major variables: (1) latitude, (2) stability class, and (3) NO $_x$ emission rate. Table 3 lists the simulation conditions for the ship-plume photochemical/dynamic modeling. As shown in Table 3, the ship-track situations at the three latitudes were considered in order to examine the extent of the

Elevated HCHO levels in the ship-going MBL

C. H. Song et al.

Title Page

Abstract

Introduction

Conclusions

References

Tables

Figures

◀

▶

◀

▶

Back

Close

Full Screen / Esc

Printer-friendly Version

Interactive Discussion



increase in the HCHO levels (or the degree of activity of the HCHO-related photochemistry in the ship-going MBL): (1) tropical, (2) sub-tropical, and (3) mid-latitude regions. The three latitudinal situations were constructed considering three busy ship-traffic corridors: (1) between Sri Lanka and Sumatra (5° N; 90° E); (2) between Singapore and Taiwan (27° N; 127° E, near Taiwan, a polluted background situation); and (3) between Tokyo and San Francisco (48° N; 165° E, near Japan) over the western Pacific ocean (referring to Automated Mutual-assistance Vessel Rescue system (AMVER), <http://www.amver.com/density.asp>. The data for the background composition in Table 3 was obtained from various measurements and global CTM simulation, such as NASA/GTE PEM-West A & B and Trace-P campaigns and GEOS-CHEM modeling (Chin et al., 2000; de Gouw et al., 2001; Kamra et al., 2001; Arnold et al., 2009). The details are shown in the footnote of Table 3.

Basically twelve scenario simulations were carried out at each latitude, changing the MBL stability conditions from neutral to stable (i.e., stability classes of D, E, and F) and NO_x emission rates from 3 to 12 g s⁻¹ (i.e., 3, 6, 9, and 12 g s⁻¹). Numbering for the 12 scenarios was made sequentially from scenarios I-a to III-d (regarding the numbering convention, refer to the footnote of Table 4). The simulations at each latitude were extended further to account for seasonal variations in the HCHO-related photochemistry by carrying out the simulations at four Julian days of 80, 173, 267, and 356, which correspond to the spring equinox, summer solstice, fall equinox, and winter solstice in the Northern Hemisphere, respectively. Therefore, a total of forty eight simulations were carried out at each latitude, and the results are summarized in Table 4. While constructing the scenarios, the changes in the primary NMVOC emissions were excluded, based on our discussions in Sect. 3.1. The $J(\text{O}_3)$ values for the photolysis reaction of $\text{O}_3 + h\nu \rightarrow \text{O}(^1\text{D}) + \text{O}_2$ are presented in Table 3 to show the latitudinal variations in the intensity of solar radiation because the differences in the magnitudes of $J(\text{O}_3)$ lead to different OH levels. As shown in Table 3, a more polluted background situation was selected for the sub-tropical conditions than for tropical conditions, with an intention of examining the main factor to affect the degree of activity of the HCHO-related photo-

**Elevated HCHO levels
in the ship-going
MBL**C. H. Song et al.

[Title Page](#)[Abstract](#)[Introduction](#)[Conclusions](#)[References](#)[Tables](#)[Figures](#)[⏪](#)[⏩](#)[◀](#)[▶](#)[Back](#)[Close](#)[Full Screen / Esc](#)[Printer-friendly Version](#)[Interactive Discussion](#)

chemistry in the ship-going MBL.

To examine the extent of the enhancements in the HCHO levels (or the degree of activity of the HCHO-related photochemistry), one variable, the maximum difference of HCHO mixing ratio ($\Delta[\text{HCHO}]_{\text{max}}$) between peak HCHO level ($[\text{HCHO}]_{\text{peak}}$) inside the ship plume and background HCHO level ($[\text{HCHO}]_{\text{back}}$), was chosen from the scenario simulations, i.e.:

$$\Delta[\text{HCHO}]_{\text{max}} = [\text{HCHO}]_{\text{peak}} - [\text{HCHO}]_{\text{back}} \quad (6)$$

Table 4 lists the model-calculated maximum differences for the scenarios. In the scenario simulations, all the first plume puffs were released at 10:30 a.m. LST. Therefore, the peak OH values appeared around noon, after a period of ozone/OH/HCHO depletions. In addition, this is the approximate local pass time of the ESA/ERS-2 GOME satellite sensor (Marbach et al., 2009). This release time was chosen intentionally considering satellite studies.

The background HCHO levels in this study were again calculated by UBoM 2K8 modeling using the method discussed in Sect. 2.2. Table 3 lists the calculated background HCHO mixing ratios. The background HCHO mixing ratios are lower than those reported by Wagner et al. (2001). Again, the background HCHO mixing ratios are affected greatly by the background NMVOC levels, and are most sensitive to the isoprene levels (Wagner et al., 2002). However, such levels are highly variable due to their short atmospheric lifetimes. For example, the calculated background HCHO mixing ratios have a higher value (98.0 pptv) in sub-tropical regions despite the less intense solar intensity compared to tropical regions (78.0 pptv). This is because a more polluted background situation in terms of the O_3 and NMVOC mixing ratios was chosen for the sub-tropical conditions, as mentioned previously. The high levels of O_3 and NMVOCs in the sub-tropical background air enhance the levels of the “background HCHO”.

In addition, the peak HCHO mixing ratios within the ship plumes can also be estimated by adding the calculated background HCHO levels to the differences in HCHO mixing ratios ($\Delta[\text{HCHO}]_{\text{max}}$) (refer to Eq. 6). Table 4 shows the differences in HCHO

Elevated HCHO levels in the ship-going MBL

C. H. Song et al.

Title Page

Abstract

Introduction

Conclusions

References

Tables

Figures

⏪

⏩

◀

▶

Back

Close

Full Screen / Esc

Printer-friendly Version

Interactive Discussion



UBoM 2K8 model with relatively low background conditions, which are not affected directly by other ship emissions in the narrow ship track. The real background HCHO mixing ratios could be much higher than the ones used in this study due to the effects of the pollutants emitted from other ships in the heavy ship traffic background.

3.3 Remaining uncertainties

CH₄ oxidation and HCHO production within ship plumes were examined using a ship-plume photochemical/dynamic model. Although the ship-plume model used in this study is equipped with state-of-the-science chemical schemes, aerosol micro-physics and dynamics, and heterogeneous reaction parameterizations, it does not include several HCHO-related chemical and heterogeneous processes, e.g.: (1) HCHO uptake by marine aerosols with the production of organic complexes or formic acid (e.g., Jacob et al., 1996; Kieber et al, 1999); (2) heterogeneous recycling of CH₃OH to HCHO on the surface of marine aerosols (Jaegle et al., 2000); and (3) halogen chemistry (Sander and Crutzen, 1996; Vogt et al., 1996; Wagner et al., 2002; von Glasow et al., 2003). The heterogeneous HCHO uptake and recycling of CH₃OH to HCHO were excluded because these issues are rather speculative without any concrete evidence from the field measurements. In addition, as discussed in Sect. 3.1, the formation of CH₃OH would be limited at high NO_x situations. Therefore, the heterogeneous recycling of CH₃OH was excluded.

Halogen chemistry is often active in the MBL and could also be important in ship plumes. If halogen chemistry is active in the ship-influenced MBL, the rate of CH₄ oxidation (rate of hydrogen abstract by Cl, i.e., CH₄+Cl+O₂ → CH₃O₂+HCl) and the rate of the CH₃O₂+XO → HCHO+X+HO₂ (where X=Cl, Br, or I) reaction could be enhanced further, yielding even higher HCHO mixing ratios in the ship-going MBL. However, under high NO_x conditions, such as ship plumes, bromine chemistry may be of limited importance as BrO mixing ratios might be reduced. In the early plume this can be caused by the reaction NO+BrO → NO₂+Br (von Glasow et al., 2003). It can also be caused by radical termination reactions of BrO+NO₂ → BrONO₂. On the

Elevated HCHO levels in the ship-going MBL

C. H. Song et al.

Title Page

Abstract

Introduction

Conclusions

References

Tables

Figures

◀

▶

◀

▶

Back

Close

Full Screen / Esc

Printer-friendly Version

Interactive Discussion



**Elevated HCHO levels
in the ship-going
MBL**

C. H. Song et al.

Title Page

Abstract

Introduction

Conclusions

References

Tables

Figures

◀

▶

◀

▶

Back

Close

Full Screen / Esc

Printer-friendly Version

Interactive Discussion



other hand, the formation of BrONO_2 can lead to an increase in the release of bromine from sea-salt aerosol as the very photolabile Br_2 is released from sea-salt aerosol upon the reaction of BrONO_2 on bromide containing aerosol (see discussion in Sander et al., 1999). The magnitude of reaction probability of BrONO_2 on sea-salt particles ($\gamma_{\text{BrONO}_2, \text{SS}}$) is somewhat uncertain but Sander et al. (1999) showed that this reaction can be important for an order of $\gamma_{\text{BrONO}_2, \text{SS}}$ of 0.8.

Although the efficiency of the auto-catalytic bromine release from sea-salt particles under the high NO_x ship-plume conditions is somewhat uncertain and its effect on HCHO is probably limited, it is still likely that chlorine atoms play an active role in the ship-plume photochemistry, especially for the oxidation of CH_4 . Enhanced concentrations of chlorine in ship plumes can result from acid displacement of HCl from sea-salt aerosol and subsequent release of Cl atoms upon the reaction of HCl with OH (see e.g., Keene et al., 2007). Another pathway for chlorine release is via the reaction of dinitrogen pentoxide (N_2O_5) on chloride containing aerosol particles, resulting in the formation of nitryl chloride (ClNO_2) which decomposes to Cl atoms and NO_2 at daytime (Osthoff et al., 2008; von Glasow, 2008). Figure 8 shows the build-up of N_2O_5 in the ITCT 2K2 base ship-plume case, even during daytime situations due to the high levels of NO_2 and O_3 (a detailed analysis regarding the daytime N_2O_5 formation inside the ship plumes was reported by Song et al. (2003a)). At this stage, the predicted N_2O_5 concentrations have not been confirmed by measurements, so that a reliable quantification of a potential Cl atom source from this mechanism is difficult. The rate constant for $\text{CH}_4 + \text{Cl}$ is about 17 times faster than $\text{CH}_4 + \text{OH}$ (at $T=290\text{ K}$), in order for Cl atoms to contribute 10% to the oxidation of CH_4 under the high OH conditions in ship plumes as predicted in this study. For this condition, Cl concentrations would have to be on the order of $[\text{Cl}] = 6 \times 10^5$ (atoms cm^{-3}).

4 Summary and future studies

Enhanced levels of formaldehyde (HCHO) along global ship corridors were observed from satellite sensors and predicted using global 3-D chemistry-transport models. Three likely sources were investigated to identify the detailed sources of the enhanced levels of HCHO in the ship corridors: (1) primary HCHO emission from ships, (2) secondary HCHO production from NMVOCs emitted from ships, and (3) atmospheric oxidation of CH₄. By carrying out multiple ship-plume model runs, it was found that CH₄ oxidation via enhanced levels of OH radicals is mainly responsible for the elevated levels of HCHO inside the ship plumes. After an average of ~200 min after the release of ship plumes, more than ~91% of the HCHO enhancements within the ship plumes was produced by this atmospheric chemical process for the ITCT 2K2 base case. Various likely ship-plume situations in the global ship corridors were also studied to determine the extent of the enhancements of the HCHO levels in the ship-going MBL. It was found that the ship-plume HCHO levels could increase up to ~434.9 pptv higher than the background HCHO levels, depending on the latitudinal location of ship plumes, NO_x emission rates and the stability of the MBL.

As demonstrated in this study and Kim et al.'s work (2009), the enhanced OH levels inside the ship-plume results in elevated levels of HCHO as well as acidic substances, such as HNO₃ and H₂SO₄, mainly through the oxidation of ship-emitted NO₂ and SO₂. Within the heavy ship-traffic MBL over the oceans, the active production of HNO₃ and H₂SO₄ can lead to increased formation of particulate nitrate and sulfate, both of which have a negative impact on the global radiative forcing (Hansen and Sato, 2001; IPCC 2007). In addition, the increased H₂SO₄ mixing ratios within the ship plumes can create favorable conditions for fresh particle formation (i.e., nucleation), which can subsequently grow into accumulation-mode particles and can often form stratocumulus clouds, known for "ship track" (e.g., Radke et al., 1989; Song et al., 2003b; Frick and Hoppel, 2000; Hobbs et al., 2000; Hudson et al., 2000; Phinney et al., 2009). Furthermore, when particulate nitrate in the MBL ship corridor is dry-deposited

Elevated HCHO levels in the ship-going MBL

C. H. Song et al.

Title Page

Abstract

Introduction

Conclusions

References

Tables

Figures

◀

▶

◀

▶

Back

Close

Full Screen / Esc

Printer-friendly Version

Interactive Discussion



Elevated HCHO levels in the ship-going MBL

C. H. Song et al.

Title Page

Abstract

Introduction

Conclusions

References

Tables

Figures

◀

▶

◀

▶

Back

Close

Full Screen / Esc

Printer-friendly Version

Interactive Discussion



5 onto the ocean surface, it acts as a fertilizer (nitrogen source) that can subsequently increase the active phytoplankton activity in the ocean (Duce et al., 1991; Prospero et al., 1996; Dentener et al., 2006; Duce et al., 2008). Such active phytoplankton activities could enable ocean surface to take up more CO₂ from the atmosphere, which would enhance the DMS fluxes from the ocean surface. Both processes would lead to global cooling (Charlson et al., 1987; Cropp et al., 2007). Overall, the immense influences of ship-plume photochemistry on atmospheric chemical cycles, global climate changes and marine biota activities as well as the complicated interactions between these changes should be investigated further with a more comprehensive and multi-disciplinary research framework, such as European Surface Ocean-Lower Atmosphere Study (SOLAS) (<http://www.solas-int.org>).

15 *Acknowledgement.* This study was funded by the Korea Meteorological Administration Research and Development Program under Grant CATER 2006–3201 in Korea. C. H. Song was on his sabbatical leave in the School of Environmental Sciences at the University of East Anglia (UEA), UK. All the ITCT 2K2 airborne data sets in this study were obtained from the official NOAA data archive at <http://esrl.noaa.gov/csd/tropchem/2002ITCT/P3/DataDownload/index.php>.

References

- 20 Arnold, S. R., Spracklen, D. V., Williams, J., Yassaa, N., Sciare, J., Bonsang, B., Gros, V., Peeken, I., Lewis, A. C., Alvain, S., and Moulin, C.: Evaluation of the global oceanic isoprene source and its impacts on marine organic carbon aerosol, *Atmos. Chem. Phys.*, 9, 1253–1262, doi:10.5194/acp-9-1253-2009, 2009.
- Bey, I., Jacob, D. J., Yantosca, R. M., Logan, J. A., Field, B. D., Fiore, A. M., Li, Q., Liu, H. Y., Mickley, L. J., and Schultz, M. G.: Global modeling of tropospheric chemistry with assimilated meteorology: Model description and evaluation, *J. Geophys. Res.*, 106, 23073–23096, 2001.
- 25 Capaldo, K., Corbett, J. J., Kasibhatla, P., Fischbeck, P., and Pandis, S. N.: Effects of ship emissions on sulphur cycling and radiative climate forcing over the ocean, *Nature*, 400, 743–746. 1999.

Elevated HCHO levels in the ship-going MBL

C. H. Song et al.

Title Page

Abstract

Introduction

Conclusions

References

Tables

Figures

◀

▶

◀

▶

Back

Close

Full Screen / Esc

Printer-friendly Version

Interactive Discussion



- Charlson, R. J., Lovelock, J. E., Andreae, M. O., and Warren, S. G.: Oceanic phytoplankton, atmospheric sulfur, cloud albedo and climate, *Nature*, 326, 655–661, 1987.
- Chen, G., Huey, L. G., Trainer, M., Nicks, D., Corbett, J., Ryerson, T., Parrish, D., Neuman, J. A., Nowak, J., Tanner, D., Holloway, J., Brock, C., Crawford, J., Olson, J. R., Sullivan, A., Weber, R., Schauffler, S., Donnelly, S., Atlas, E., Roberts, J., Flocke, F., Hübler, G., and Fehsenfeld, F.: An investigation of the chemistry of ship emission plumes during ITCT 2002, *J. Geophys. Res.*, 110, D10S90, doi:10.1029/2004JD005236, 2005.
- Chin, M., Rood, R. B., Lin, S.-J., Müller, J.-F., and Thompson, A. M.: Atmospheric sulfur cycle simulated in the global model GOCART: Model description and global properties, *J. Geophys. Res.*, 110(D20), 24671–24687, 2000.
- Cooper, D. A., Peterson, K., and Simpson, D.: Hydrocarbon, PAH and PCB emissions from ferries: A case study in the Skagerak-Kattegat-Öresund region, *Atmos. Environ.*, 30(14), 2463–2473, 1996.
- Corbett, J. J. and Fischbeck, P.: Emissions from ships, *Science*, 278, 823–824, 1997.
- Corbett, J. J., Fischbeck, P. S., and Pandis, S. N.: Global nitrogen and sulfur inventories for oceangoing ships, *J. Geophys. Res.*, 104(D3), 3457–3470, 1999.
- Corbett, J. J. and Koehler, H. W.: Updated emissions from ocean shipping, *J. Geophys. Res.*, 108(D20), 4650, doi:10.1029/2003JD003751, 2003.
- Cropp, R., Norbury, J., and Braddock, R.: Dimethylsulfide, clouds, and phytoplankton: Insight from a simple plankton ecosystem feedback model, *Global Biogeochem. Cy.*, 21, 21(GB2024), doi:10.1029/2006GB002812, 2007.
- de Gouw, J. A., Warneke, C., Scheeren, H. A., van der Veen, C., Bolder, M., Scheele, M. P., Williams, J., Wong, S., Lange, L., Fischer, H., and Lelieveld, J.: Overview of the trace gas measurements on board the Citation aircraft during the intensive field phase of INDOEX, *J. Geophys. Res.*, 106(D22), 28453–28467, 2001.
- Dentener, F., Drevet, J., Lamarque, J. F., et al.: Nitrogen and sulfur deposition on regional and global scales: A multimodel evaluation, *Global Biogeochem. Cy.*, 20(5), 20(GB4003), doi:10.1029/2005GB002672, 2006.
- Duce, R. A., Liss, P. S., Merrill, J. T., et al.: The atmospheric input of trace species to the world ocean, *Global Biogeochem. Cy.*, 5(3), 193–259, 1991.
- Duce, R. A., Roche, J. L., Altieri, K., et al.: Impacts of atmospheric anthropogenic nitrogen on the open ocean, *Science*, 320, 893–897, 2008.
- Endresen, Ø., Sørsgård, E., Sundet, J. K., Dalsøren, S. B., Isaksen, I. S. A., Berglen, T. F.,

Elevated HCHO levels in the ship-going MBL

C. H. Song et al.

Title Page

Abstract

Introduction

Conclusions

References

Tables

Figures

◀

▶

◀

▶

Back

Close

Full Screen / Esc

Printer-friendly Version

Interactive Discussion



and Gravir, G.: Emission from international sea transportation and environmental impact, *J. Geophys. Res.*, 108(D17), 4560, doi:10.1029/2002JD002898, 2003.

European Commission Directorate General Environment and Entec UK Ltd.: Service Contract on Ship Emissions: Assignment, Abatement and Market-based Instruments. Task 1- Preliminary Assignment of Ship Emissions to European Countries, London, 2005.

EPA: Analysis of Commercial Marine Vessels Emissions and Fuel Consumption Data, Technical Report EPA 420-R-00-002, US EPA, 2000.

Eyring, V., Stevenson, D. S., Lauer, A., Dentener, F. J., Butler, T., Collins, W. J., Ellingsen, K., Gauss, M., Hauglustaine, D. A., Isaksen, I. S. A., Lawrence, M. G., Richter, A., Rodriguez, J. M., Sanderson, M., Strahan, S. E., Sudo, K., Szopa, S., van Noije, T. P. C., and Wild, O.: Multi-model simulations of the impact of international shipping on Atmospheric Chemistry and Climate in 2000 and 2030, *Atmos. Chem. Phys.*, 7, 757–780, doi:10.5194/acp-7-757-2007, 2007.

Faloon, I.: Sulfur processing in the marine atmospheric boundary layer: A review and critical assessment of modeling uncertainties, *Atmos. Environ.*, 43, 2841–2854, 2009.

Finlayson-Pitts, B. J. and Pitts Jr., J. N.: *Chemistry of the Upper and Lower Atmosphere: Theory, Experiment, and Applications*, Academic Press, San Diego, California, USA, 2000.

Frick, G. M. and Hoppel, W. A.: Airship measurements of ship's exhaust plumes and their effect on marine boundary layer clouds, *J. Atmos. Sci.*, 57, 2625–2648, 2000.

Hanna, S. R., Schulman, L. L., Paine, R. J., Pleim, J. E., and Baer, M.: Development and evaluation of the offshore and coastal dispersion model, *J. Air Pollut. Control Assoc.*, 35, 1039–1047, 1985.

Hansen, J. E. and Sato, M.: Trends of measured climate forcing agents, *Proc. Natl. Acad. Sci.*, 98(26), 14778–14783, 2001.

Hobbs, P. V., Garrett, T. J., Ferek, R. J., Strader, S. R., Hegg, D. A., Frick, G. M., Hoppel, W. A., Gasparovic, R. F., Russell, L. M., Johnson, D. W., O'Dowd, C., Durkee, P. A., Nielsen, K. E., and Innis, G.: Emissions from ships with respect to their effects on clouds, *J. Atmos. Sci.*, 57, 2570–2590, 2000.

Houyoux, M.: Clean Air Interstate Rule Emissions Inventory Technical Support Document, US EPA, 2005.

Hoor, P., Borken-Kleefeld, J., Caro, D., Dessens, O., Endresen, O., Gauss, M., Grewe, V., Hauglustaine, D., Isaksen, I. S. A., Jöckel, P., Lelieveld, J., Myhre, G., Meijer, E., Olivie, D., Prather, M., Schnadt Poberaj, C., Shine, K. P., Staehelin, J., Tang, Q., van Aardenne, J., van

**Elevated HCHO levels
in the ship-going
MBL**

C. H. Song et al.

Title Page

Abstract

Introduction

Conclusions

References

Tables

Figures

◀

▶

◀

▶

Back

Close

Full Screen / Esc

Printer-friendly Version

Interactive Discussion



Velthoven, P., and Sausen, R.: The impact of traffic emissions on atmospheric ozone and OH: results from QUANTIFY, *Atmos. Chem. Phys.*, 9, 3113–3136, doi:10.5194/acp-9-3113-2009, 2009.

Hudson, J. G., Garrett, T. J., Hobbs, P. V., Strader, S. R., Xie, Y., and Yum, S. S.: Cloud condensation nuclei and ship tracks, *J. Atmos. Sci.*, 57, 2696–2706, 2000.

Intergovernmental Panel on Climate Change (IPCC): *Climate Change 2007: The Physical Science Basis, the Fourth Assessment Report of the IPCC*, ISBN 978052188009-1, 2007.

Jacob, D. J., Heikes, B. G., Fan, S. M., et al.: Origin of ozone and NO_x in the tropical troposphere: A photochemical analysis of aircraft observations over South Atlantic basin, *J. Geophys. Res.*, 101, 24235–24250, 1996.

Jaenicke, R.: *Tropospheric Aerosols*, edited by: Hobbs, P. V., Academic Press, San Diego, California, 1–31, 1993

Jaegle, L., Jacob, D. J., Brune, W. H., et al.: Photochemistry of HO_x in the upper troposphere at the northern midlatitudes, *J. Geophys. Res.*, 105, 3877–3892, 2000.

Kamra, A. K., Murugavel, P., Pawar, S. D., and Gopalakrishnan, V.: Background aerosol concentration derived from the atmospheric electric conductivity measurements made over the Indian Ocean during INDOEX, *J. Geophys. Res.*, 106(D22), 28643–28651, 2001.

Karlsdóttir, S. and Isaksen, I. S. A.: Changing methane lifetime: Possible cause for reduced growth, *Geophys. Res. Lett.*, 27(1), 93–96, 2000.

Kasibhatla, P., Levy II, H., Moxim, W. J., Pandis, S. N., Corbett, J. J., Peterson, M. C., Honrath, R. E., Frost, G. J., Knapp, K., Parrish, D. D., and Ryerson, T. B.: Do emissions from ship have a significant impact on concentrations of nitrogen oxides in the marine boundary layer? *Geophys. Res. Lett.*, 27, 2229–2232, 2000.

Keene, W. C., Stutz, J., Pszenny, A. A. P., Maben, J. R., Fisher, E. V., Smith, A. M., von Glasow, R., Pechtl, S., Sive, B. C., and Varner, R. K.: Inorganic chlorine and bromine in coastal New England air during summer, *J. Geophys. Res.*, 112, D10S12, doi:10.1029/2006JD007689, 2007

Kieber, R. J., Rhines, M. F., Willey, J. D., and Avery Jr., G. B.: Rainwater formaldehyde: Concentration, deposition, and photochemical formation, *Atmos. Environ.*, 33, 3659–3667, 1999.

Kim, H. S., Song, C. H., Park, R. S., Huey, G., and Ryu, J. Y.: Investigation of ship-plume chemistry using a newly-developed photochemical/dynamic ship-plume model, *Atmos. Chem. Phys.*, 9, 7531–7550, doi:10.5194/acp-9-7531-2009, 2009.

Lawrence, M. G. and Crutzen, P. J.: Influence of NO_x emissions from ships on tropospheric

**Elevated HCHO levels
in the ship-going
MBL**C. H. Song et al.

[Title Page](#)[Abstract](#)[Introduction](#)[Conclusions](#)[References](#)[Tables](#)[Figures](#)[◀](#)[▶](#)[◀](#)[▶](#)[Back](#)[Close](#)[Full Screen / Esc](#)[Printer-friendly Version](#)[Interactive Discussion](#)

photochemistry and climate, *Nature*, 402, 167–170, 1999.

Lawrence, M. G., Jöckel, P., and von Kuhlmann, R.: What does the global mean OH concentration tell us?, *Atmos. Chem. Phys.*, 1, 37–49, doi:10.5194/acp-1-37-2001, 2001.

Lloyd's Register: Marine Exhaust Emissions Research Programme, Lloyd's Register Eng. Serv., London, 1995

Lurmann, F. W., Lloyd, A. C., and Atkinson, R.: A chemical mechanism for use in long-range transport/acid deposition computer modeling, *J. Geophys. Res.*, 91(D10), 10905–10936, 1986.

Marbach, T., Beirle, S., Platt, U., Hoor, P., Wittrock, F., Richter, A., Vrekoussis, M., Grzegorski, M., Burrows, J. P., and Wagner, T.: Satellite measurements of formaldehyde linked to ship-going emissions, *Atmos. Chem. Phys.*, 9, 8223–8234, doi:10.5194/acp-9-8223-2009, 2009.

Osthoff, H. D., Roberts, J. M., Ravishankara, A. R., et al.: High levels of nitryl chloride in the polluted subtropical marine boundary layer, *Nature Geosci.*, 1, 324–328, 2008.

Parrish, D. D., Kondo, Y., Cooper, O. R., Brock, C. A., Jaffe, D. A., Trainer, M., Ogawa, T., Hübler, G., and Fehsenfeld, F. C.: Intercontinental Transport and Chemical Transformation 2002 (ITCT 2K2) and Pacific Exploration of Asian Continental Emission (PEACE) experiments: An overview of the 2002 winter and spring intensives, *J. Geophys. Res.*, 109, D23S01, doi:10.1029/2004JD004980, 2004.

Langley, L., Leaitch, W. R., Lohmann, U., Shantz, N. C., and Worsnop, D. R.: Contributions from DMS and ship emissions to CCN observed over the summertime North Pacific, *Atmos. Chem. Phys.*, 10, 1287–1314, doi:10.5194/acp-10-1287-2010, 2010.

Prospero, J. M., Barrett, K., Church, T., et al.: Atmospheric deposition of nutrients to the North Atlantic Basin, *Biogeochemistry*, 35(1), 27–73, 1996.

Radke, L. F., Coakley Jr., J. A., and King, M. D.: Direct and remote sensing observations of the effects of ships on clouds, *Science*, 246, 1146–1149, 1989.

Sander, R. and Crutzen, P. J.: Model study indicating halogen activation and ozone destruction in polluted air masses transported to the sea, *J. Geophys. Res.*, 101(D4), 9121–9138, 1996.

Sander, R., Rudich, Y., von Glasow, R., and Crutzen, P. J.: The role of BrNO₃ in marine tropospheric chemistry: A model study, *Geophys. Res. Lett.*, 226, 2857–2860, 1999.

Song, C. H., Chen, G., Hanna, S. R., Crawford, J., and Davis, D. D.: Dispersion and chemical evolution of ship plumes in the marine boundary layer: Investigation of O₃/NO_y/HO_x chemistry, *J. Geophys. Res.*, 108(D4), 4143, doi:10.1029/2002JD002216, 2003a.

Song, C. H., Chen, G., and Davis, D. D.: Chemical evolution and dispersion of ship plumes

in the remote marine boundary layer: Investigation of sulfur chemistry, *Atmos. Environ.*, 37, 2663–2679, 2003b.

Song, C. H., Han, K. M., Cho, H. J., Kim, J., Carmichael, G. R., Kurata, G., Thongboonchoo, N., He, Z., and Kim, H. S.: A Lagrangian model investigation of chemico-microphysical evolution of northeast Asian pollution plumes within the MBL during Trace-P, *Atmos. Environ.*, 41, 8932–8951, 2007.

Tuan, M. D.: Eulerian photochemical box modeling for investigating secondary inorganic formation over the greater Seoul area, MS thesis, GIST, Gwangju, 2008.

Xuan, N. T.: Measured and modeled ozone production efficiency along the Pacific coast of North America, M.Sc. thesis, GIST, Gwangju, 2009.

Vogt, R., Crutzen, P. J., and Sander, P. J.: A mechanism for halogen release from sea-salt aerosol in the remote marine boundary layer, *Nature*, 383, 327–330, 1996.

von Glasow, R., Lawrence, M. G., Sander, R., and Crutzen, P. J.: Modeling the chemical effects of ship exhaust in the cloud-free marine boundary layer, *Atmos. Chem. Phys.*, 3, 233–250, doi:10.5194/acp-3-233-2003, 2003.

von Glasow, R.: Pollution meets sea-salt, *Nature Geosci.*, 1, 292–293, 2008.

Wagner, V., Schiller, C., and Fischer, H.: Formaldehyde measurements in the marine boundary layer of the Indian Ocean during the 1999 INDOEX cruise of the RV Ronald H. Brown, *J. Geophys. Res.*, 106, 28529–28538, 2001.

Wagner, V., von Glasow, R., Fischer, H., and Crutzen, P. J.: Are CH₂O measurements in the marine boundary layer suitable for testing the current understanding of the CH₄ photooxidation?: A model study, *J. Geophys. Res.*, 107(D3), doi:10.1029/2001JD000722, 2002.

ACPD

10, 15441–15483, 2010

Elevated HCHO levels in the ship-going MBL

C. H. Song et al.

Title Page

Abstract

Introduction

Conclusions

References

Tables

Figures

◀

▶

◀

▶

Back

Close

Full Screen / Esc

Printer-friendly Version

Interactive Discussion



Elevated HCHO levels in the ship-going MBL

C. H. Song et al.

Title Page

Abstract

Introduction

Conclusions

References

Tables

Figures

◀

▶

◀

▶

Back

Close

Full Screen / Esc

Printer-friendly Version

Interactive Discussion



Table 1. Estimated ranges of the NMVOC mass-fractions and emission rates from ships^a.

NMVOCs ^b	Range of mass fraction
Ethane	0.001–0.024
Ethene	0.043–0.140
Formaldehyde ^c	0.040–0.100
Propane	0.000–0.002
Higher alkanes ^d	0.161–0.619
Higher alkenes ^e	0.030–0.111
Aromatics ^f	0.099–0.277
Benzene	0.108–0.184
Total NMVOC emission rate (g/s) ^g	0.09–0.93

^a The mass fractions of NMVOCs species were estimated based on EPA (2002), Endersen et al. (2003), European Commission Directorate General Environment And Entec UK Limited (2005), and Houyoux (2005).

^b Chemical speciation was based on Cooper et al. (1996).

^c The fraction of HCHO was assumed to be from 4% to 10% of the total NMVOC emissions (Houyoux, 2005; Marbach et al., 2009). 10% is the upper-limit.

^d Higher alkanes represent the lumped alkane species with a carbon number >4.

^e Higher alkenes represent the lumped alkene species with carbon number >3.

^f Aromatics include branched benzene species such as toluene, xylene, styrene, etc.

^g The total NMVOC emission rates were estimated based on Endersen et al. (2003) and Entec (2005).

Elevated HCHO levels in the ship-going MBL

C. H. Song et al.

[Title Page](#)
[Abstract](#)
[Introduction](#)
[Conclusions](#)
[References](#)
[Tables](#)
[Figures](#)
[Back](#)
[Close](#)
[Full Screen / Esc](#)
[Printer-friendly Version](#)
[Interactive Discussion](#)


Table 2. Some reactions related to HCHO photochemistry in the MBL.

Reaction number	Reaction	Rate constant
(R1)	$\text{CH}_4 + \text{OH} + \text{O}_2 \rightarrow \text{CH}_3\text{O}_2 + \text{H}_2\text{O}$	k_1
(R2)	$\text{CH}_4 + \text{O}(^1\text{D}) + \text{O}_2 \rightarrow \text{CH}_3\text{O}_2 + \text{OH}$	k_2
(R3)	$\text{CH}_4 + \text{O}(^1\text{D}) \rightarrow \text{HCHO} + \text{H}_2$	k_3
(R4)	$\text{HCHO} + h\nu \rightarrow \text{CHO} + \text{H}$	J_1
(R5)	$\text{HCHO} + h\nu \rightarrow \text{CO} + \text{H}_2$	J_2
(R6)	$\text{HCHO} + \text{OH} \rightarrow \text{CHO} + \text{H}_2\text{O}$	k_4
(R7)	$\text{HCHO} + \text{NO}_3 \rightarrow \text{CHO} + \text{HNO}_3$	k_5
(R8)	$\text{HCHO} + \text{O}(^3\text{P}) \rightarrow \text{CHO} + \text{OH}$	k_6
(R9)	$\text{CH}_3\text{O}_2 + \text{HO}_2 \rightarrow \text{CH}_3\text{OOH} + \text{O}_2$	k_7
(R10)	$\text{CH}_3\text{O}_2 + \text{CH}_3\text{O}_2 \rightarrow \text{CH}_3\text{OH} + \text{HCHO} + \text{O}_2$	k_8
(R11)	$\text{CH}_3\text{O}_2 + \text{NO} \rightarrow \text{CH}_3\text{O} + \text{NO}_2$	k_9
(R12)	$\text{CH}_3\text{O} + \text{O}_2 \rightarrow \text{HCHO} + \text{HO}_2$	k_{10}

Table 3. Simulation conditions for the constructed case studies ^a

Variable	Tropical	Sub-tropical	Mid-latitude
Latitude (° N)	5	27	48
Longitude (° E)	90	127	165
Temperature (°C)	28	18	5
NO _x (pptv)	20	35	28
SO ₂ (pptv) ^b	35	26	11
O ₃ (ppbv)	18	51	42
CO (ppbv)	220	190	210
C ₂ H ₆ (ppbv)	1.00	1.70	1.81
C ₃ H ₈ (pptv) ^c	117	537	472
ALKA (pptv) ^c	29	412	245
ALKE (pptv) ^c	0.15	2.80	0.60
BENZ (pptv)	110	115	90
HCHO ^d	78.0	98.0	44.8
Isoprene (pptv) ^f	5 ^e	4 ^f	4
DMS (pptv) ^b	65	40	220
CH ₄ (ppmv)	1.80	1.80	1.82
J(O ₃) (s ⁻¹)	3.34 × 10 ⁻⁵	2.58 × 10 ⁻⁵	1.27 × 10 ⁻⁵
J(HCHO) (s ⁻¹)-a ^g	3.13 × 10 ⁻⁵	2.75 × 10 ⁻⁵	1.90 × 10 ⁻⁵
J(HCHO) (s ⁻¹)-b ^h	5.35 × 10 ⁻⁵	4.91 × 10 ⁻⁵	3.81 × 10 ⁻⁵
Aerosol surface density (μm ² /cm ³) ⁱ	42	42	42
Aerosol pH ^j	6.9	6.9	6.9

^a Background conditions for tropical, sub-tropical, and mid-latitude regions were obtained from INDOEX (de Gouw et al., 2001; Kamra et al., 2001; Wagner et al., 2002), TRACE-P, and PEM-West B airborne field campaigns (<http://www-gte.larc.nasa.gov/pem/pemb.flt.htm>).

^b Chin et al. (2000)

^c Annually-averaged mixing ratios obtained from a GEOS-CHEM simulation for the year 2005.

^d Diurnally-averaged values calculated from "Eulerian-mode" UBoM 2K8 modeling with the simulation conditions given in Table 3. The minimum and maximum background HCHO mixing ratios are 48.6 pptv–127.6 pptv, 67.8 pptv–132.3 pptv, and 31.2 pptv–63.6 pptv in tropical, sub-tropical, and mid-latitude regions, respectively.

^e Wagner et al. (2002)

^f Arnold et al. (2009), annual average values

^g $\text{HCHO} + h\nu \rightarrow \text{CHO} + \text{H}$

^h $\text{HCHO} + h\nu \rightarrow \text{CO} + \text{H}_2$

ⁱ Estimated, based on Janicke (1993).

^j Assumed, based on Song et al. (2003b).

Elevated HCHO levels in the ship-going MBL

C. H. Song et al.

Title Page

Abstract

Introduction

Conclusions

References

Tables

Figures

◀

▶

◀

▶

Back

Close

Full Screen / Esc

Printer-friendly Version

Interactive Discussion



Elevated HCHO levels in the ship-going MBL

C. H. Song et al.

[Title Page](#)
[Abstract](#)
[Introduction](#)
[Conclusions](#)
[References](#)
[Tables](#)
[Figures](#)
[⏪](#)
[⏩](#)
[◀](#)
[▶](#)
[Back](#)
[Close](#)
[Full Screen / Esc](#)
[Printer-friendly Version](#)
[Interactive Discussion](#)


Table 4. Maximum enhanced HCHO concentrations ($\Delta[\text{HCHO}]_{\text{max}}$) inside the ship plumes from the scenario simulations (unit: pptv).

Scenario	Tropical	Sub-tropical	Mid-latitude
I-a	117.9 (113.8, 121.1)	80.5 (59.2, 87.2)	41.3 (20.5, 57.8)
I-b	164.4 (158.4, 168.6)	112.3 (82.8, 121.1)	58.3 (24.6, 81.2)
I-c	195.7 (188.4, 200.5)	133.7 (98.7, 144.3)	69.9 (26.6, 97.2)
I-d	219.3 (211.2, 224.5)	149.9 (110.8, 162.0)	78.7 (27.6, 109.4)
II-a	253.2 (247.2, 257.2)	168.2 (132.5, 176.6)	94.7 (34.2, 123.4)
II-b	329.3 (320.0, 334.7)	225.5 (174.0, 237.8)	124.6 (33.9, 166.2)
II-c	371.4 (359.4, 337.7)	258.8 (193.6, 274.3)	138.5 (32.3, 191.3)
II-d	397.3 (382.3, 404.8)	280.3 (201.7, 299.6)	143.8 (32.0, 207.7)
III-a	313.6 (305.1, 319.7)	213.3 (165.9, 224.6)	118.7 (34.1, 157.1)
III-b	384.8 (371.5, 391.4)	269.9 (198.6, 287.3)	141.8 (31.6, 199.7)
III-c	415.4 (396.3, 422.9)	297.0 (201.8, 320.5)	142.5 (31.1, 220.8)
III-d	426.1 (400.3, 434.9)	309.2 (191.5, 340.5)	143.1 (30.8, 232.1)

Note 1: I, II, and III represent the MBL stability conditions of neutral (D), moderately stable (E), and stable (F), respectively, and a, b, c, and d denote the ship-plume cases with the NO_x emission rates of 3, 6, 9, and 12 g s^{-1} .

Note 2: The values were calculated under spring/fall equinox and winter/summer solstice conditions. Two figures in the parentheses represent the minimum and maximum values of the enhanced HCHO mixing ratios among the values calculated from the multiple scenario simulations.

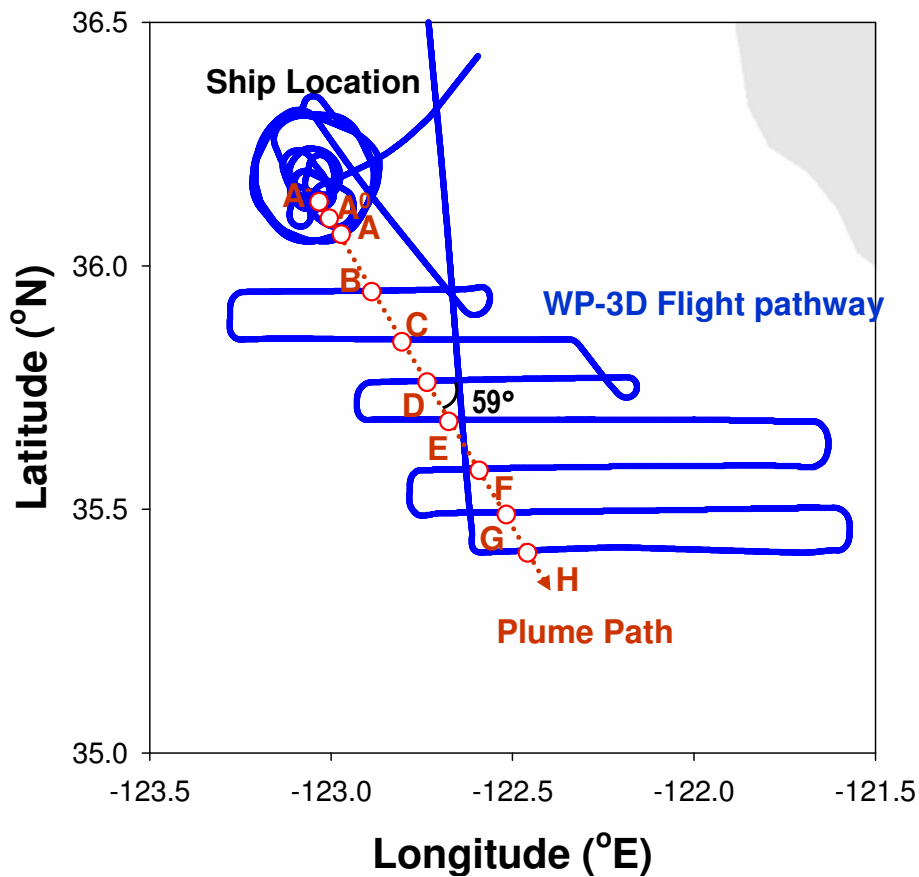


Fig. 1. Two imaginary ship-plume transects (A^- and A^0) and eight actual ship-plume transects (A–H) made by a NOAA WP-3D flight during the ITCT 2K2 campaign conducted 100 km off the California coast (Chen et al., 2005; Kim et al., 2009).

**Elevated HCHO levels
in the ship-going
MBL**

C. H. Song et al.

Title Page	
Abstract	Introduction
Conclusions	References
Tables	Figures
◀	▶
◀	▶
Back	Close
Full Screen / Esc	
Printer-friendly Version	
Interactive Discussion	



Elevated HCHO levels in the ship-going MBL

C. H. Song et al.

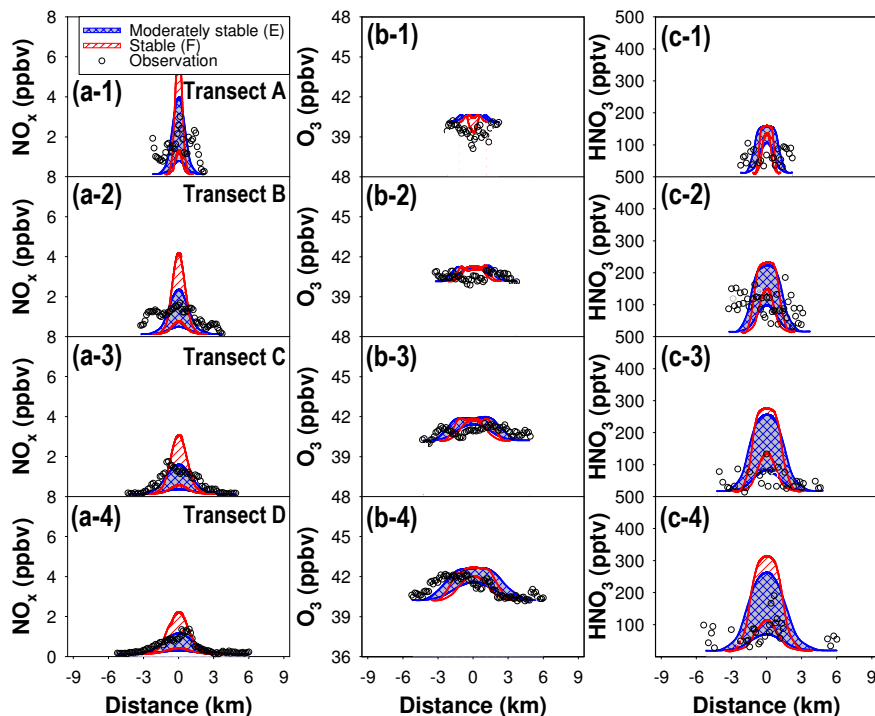


Fig. 2a. Model validations at eight transects (A–H) for NO_x , O_3 , and HNO_3 . In the model simulations, the NO_x emission rates from the ship were varied over a range of $2.6\text{--}13.3\text{ g s}^{-1}$, together with primary NMVOC and HCHO emissions.

[Title Page](#)
[Abstract](#)
[Introduction](#)
[Conclusions](#)
[References](#)
[Tables](#)
[Figures](#)
[◀](#)
[▶](#)
[◀](#)
[▶](#)
[Back](#)
[Close](#)
[Full Screen / Esc](#)
[Printer-friendly Version](#)
[Interactive Discussion](#)

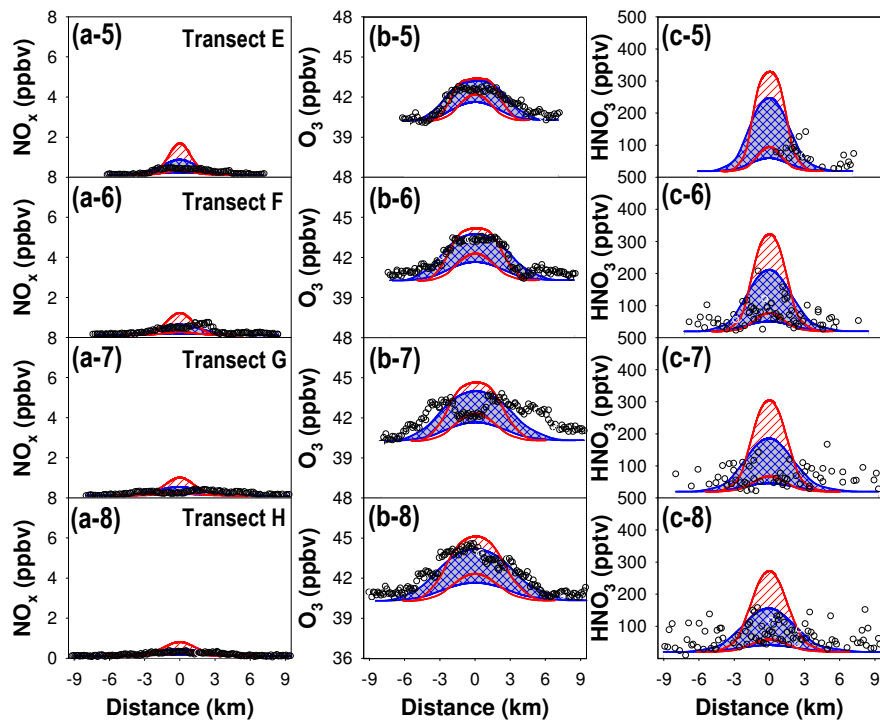



Fig. 2b. Continued.

**Elevated HCHO levels
in the ship-going
MBL**

C. H. Song et al.

Title Page

Abstract Introduction

Conclusions References

Tables Figures

◀ ▶

◀ ▶

Back Close

Full Screen / Esc

Printer-friendly Version

Interactive Discussion



Elevated HCHO levels
in the ship-going
MBL

C. H. Song et al.

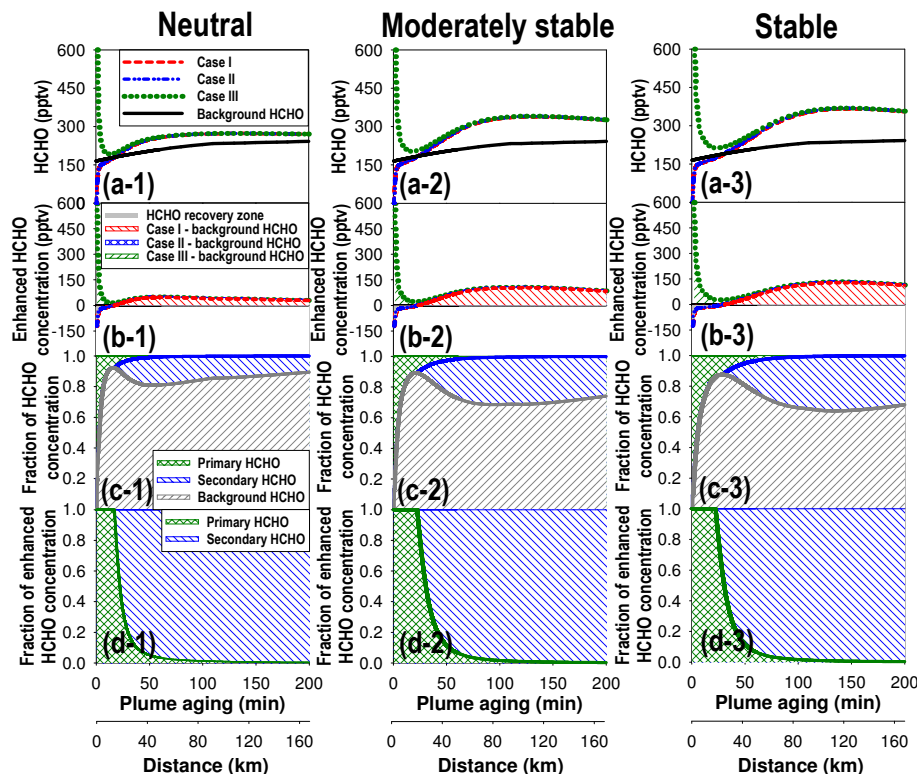


Fig. 3. HCHO sources and the budget inside the base-case ship plume (ITCT 2K2 ship-plume): **(a)** changes in the transect-averaged ship-plume HCHO mixing ratios with respect to ship-plume travel times; **(b)** differences between the transect-averaged ship-plume HCHO mixing ratios and the model-predicted background HCHO mixing ratios; **(c)** source fraction of the ship-plume HCHO mixing ratios; and **(d)** source fractions of the enhanced ship-plume HCHO mixing ratios. The first, second, and third columns show the results from the model-simulations under the conditions of neutral (D), moderately stable (E), and stable (F) MBL stability classes, respectively.

Title Page

Abstract

Introduction

Conclusions

References

Tables

Figures

◀

▶

◀

▶

Back

Close

Full Screen / Esc

Printer-friendly Version

Interactive Discussion



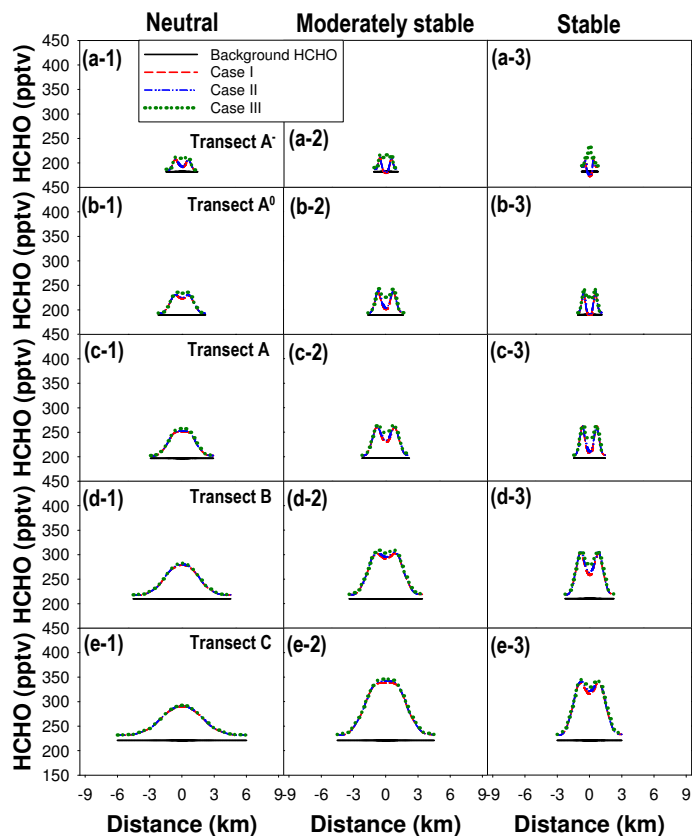


Fig. 4a. Profiles of HCHO mixing ratios inside the ITCT 2K2 ship-plume at ten transects from A⁻ to H: **(a)** transect A⁻; **(b)** transect A⁰; **(c)** transect A; **(d)** transect B; **(e)** transect C; **(f)** transect D; **(g)** transect E; **(h)** transect F; **(i)** transect G; and **(j)** transect H. The first, second, and third columns present the model-predicted profiles of the ship-plume HCHO mixing ratios under neutral (D), moderately stable (E), and stable (F) MBL conditions, respectively.

**Elevated HCHO levels
in the ship-going
MBL**

C. H. Song et al.

Title Page

Abstract

Introduction

Conclusions

References

Tables

Figures

◀

▶

◀

▶

Back

Close

Full Screen / Esc

Printer-friendly Version

Interactive Discussion



**Elevated HCHO levels
in the ship-going
MBL**

C. H. Song et al.

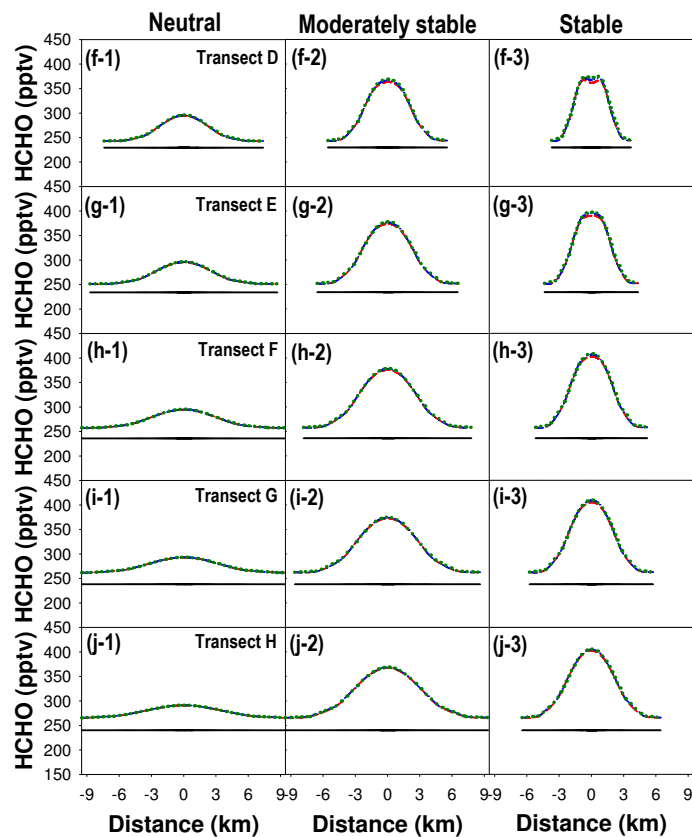


Fig. 4b. Continued.

Title Page

Abstract

Introduction

Conclusions

References

Tables

Figures

◀

▶

◀

▶

Back

Close

Full Screen / Esc

Printer-friendly Version

Interactive Discussion



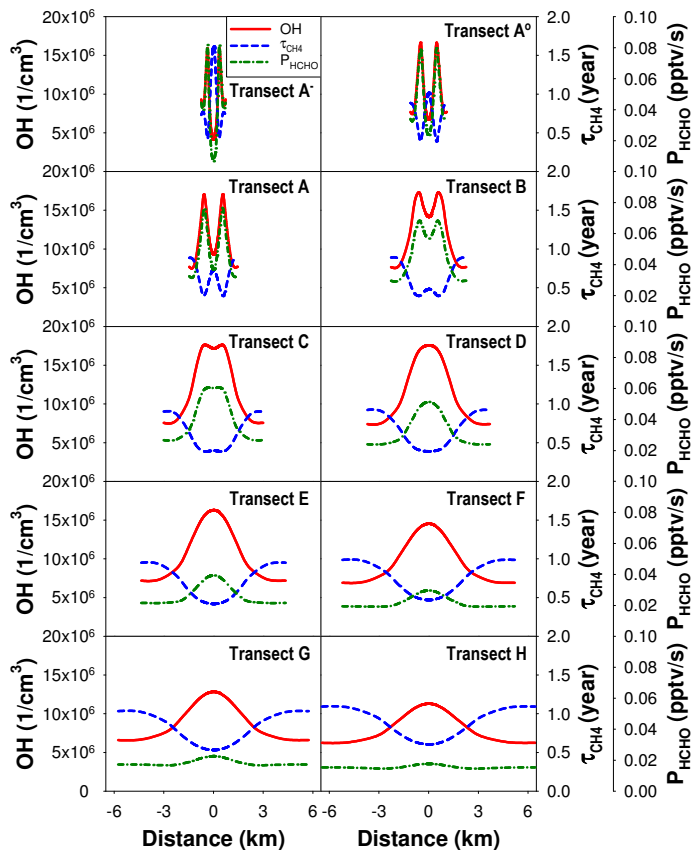


Fig. 5. Profiles of (a) OH radical concentrations, (b) instantaneous chemical lifetime of CH_4 (τ_{CH_4}), and (c) net instantaneous HCHO production rate (P_{HCHO}) at ten ship-plume transects under moderately stable MBL conditions.

Elevated HCHO levels in the ship-going MBL

C. H. Song et al.

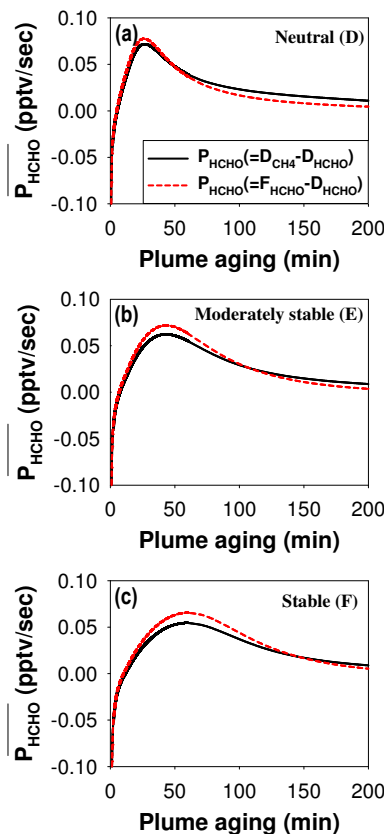


Fig. 6. Comparison between two $\overline{P_{\text{HCHO}}}$ s: (1) $D_{\text{CH}_4} - D_{\text{HCHO}}$ (black solid lines) and (2) $F_{\text{HCHO}} - D_{\text{HCHO}}$ (red dashed lines). Panels (a), (b), and (c) show the results from the simulations under the MBL conditions of neutral (D), moderately stable (E), and stable (F) classes, respectively.

[Title Page](#)
[Abstract](#)
[Introduction](#)
[Conclusions](#)
[References](#)
[Tables](#)
[Figures](#)
[◀](#)
[▶](#)
[◀](#)
[▶](#)
[Back](#)
[Close](#)
[Full Screen / Esc](#)
[Printer-friendly Version](#)
[Interactive Discussion](#)

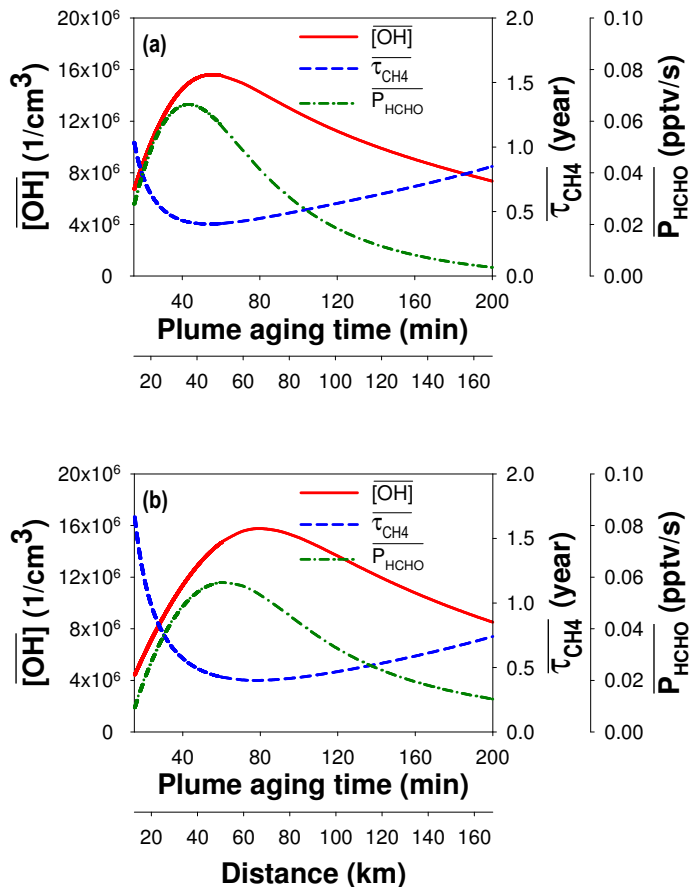



Fig. 7. Changes in the transect-averaged OH radical concentrations, instantaneous chemical lifetime of CH_4 (τ_{CH_4}), and net instantaneous HCHO production rate (P_{HCHO}) with respect to ship-plume travel time (or distance) **(a)** under moderately stable MBL condition and **(b)** under stable MBL condition.

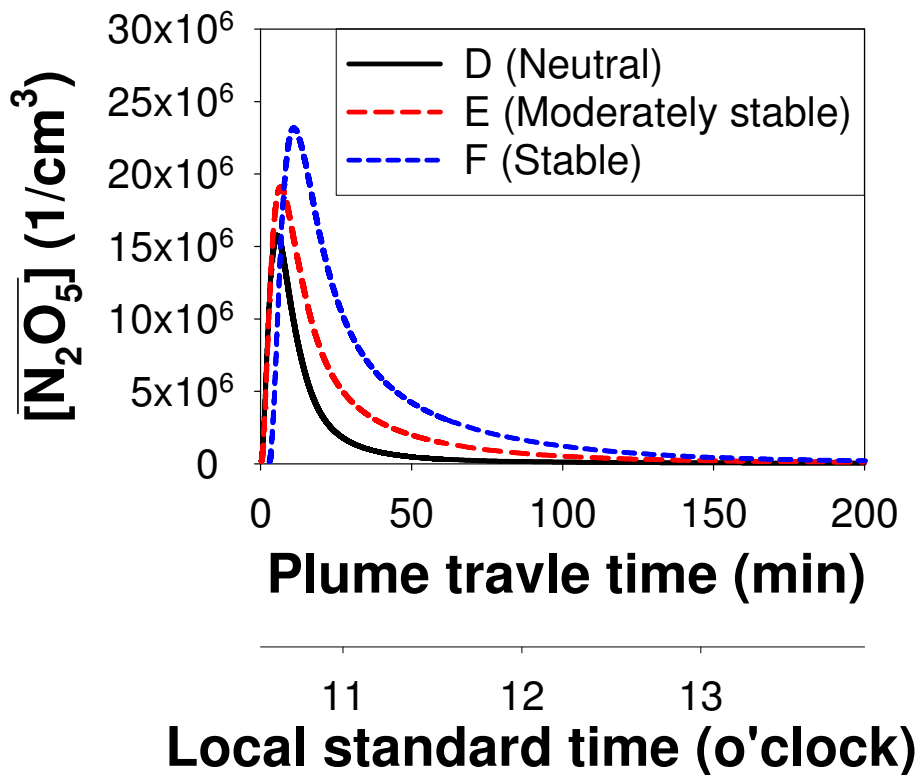


Fig. 8. Possible build-up of dinitrogen pentoxide (N_2O_5) radicals inside the ITCT 2K2 ship plume with three MBL stability classes: (i) neutral (D), (ii) moderately stable (E), and (iii) stable (F). The ship plumes are released at 10:30 a.m. LST.

**Elevated HCHO levels
in the ship-going
MBL**

C. H. Song et al.

Title Page

Abstract Introduction

Conclusions References

Tables Figures

◀ ▶

◀ ▶

Back Close

Full Screen / Esc

Printer-friendly Version

Interactive Discussion

